INSTITUTO
UNIVERSITÁRIO
DE LISBOA

Multispectral Imaging Applied to Precision Agriculture

Tiago Miguel Martins Felício

Master in Computer Engineering

Supervisor:
PhD Octavian Adrian Postolache, Full Professor,
Iscte - Instituto Universitário de Lisboa

Supervisor:
PhD Pedro Joaquim Amaro Sebastião, Full Professor,
Iscte - Instituto Universitário de Lisboa

October, 2025

TECHNOLOGY
AND ARCHITECTURE

Department of Information Science and Technology

Multispectral Imaging Applied to Precision Agriculture

Tiago Miguel Martins Felício

Master in Computer Engineering

Supervisor:
PhD Octavian Adrian Postolache, Full Professor,
Iscte - Instituto Universitário de Lisboa

Supervisor:
PhD Pedro Joaquim Amaro Sebastião, Associate Professor with aggregation,
Iscte - Instituto Universitário de Lisboa

October, 2025

Acknowledgments

I want to sincerely thank ISCTE-IUL for giving me the wonderful opportunity to learn and grow over the past five years. I am genuinely grateful for the enriching academic environment it provided.

A special thank you goes to my supervisors, Professor Octavian Adrian Postolache and Professor Pedro Joaquim Amaro Sebastião, for their guidance, encouragement, patience, and valuable feedback throughout this journey.

I also sincerely appreciate the support and resources from the staff at ISCTE-IUL and the Instituto de Telecomunicações (IT-IUL), which were essential in helping me carry out my research by providing access to equipment, libraries, and research facilities.

I am grateful to my colleagues as well, whose discussions, support, and companionship have contributed significantly to my personal and academic development.

Lastly, I want to express my heartfelt thanks to my family—especially my dad Tiago, my mom Patrícia, my younger brothers Tomás and Tomé, and my aunt Teresa—for their unconditional love, support, and encouragement. To my friends, thank you for knowing how to cheer me up when I needed it and for respecting my focus when work was in progress. Their encouragement has been the foundation that carried me through both the challenges and the successes of this journey.

Resumo

Os desafios crescentes na procura por alimentos, na variabilidade climática e na escassez de recursos evidenciaram a necessidade de soluções tecnológicas inovadoras na agricultura. Este trabalho apresenta uma plataforma de software de análise de imagens multiespectrais de terrenos agrícolas para a Agricultura de Precisão, com foco na melhoria da monitorização de culturas e na gestão de recursos.

A plataforma proposta integra dados recolhidos por Veículos Aéreos Não Tripulados (UAVs) equipados com sensores multiespectrais para avaliar a saúde da vegetação por meio de índices de vegetação (VIs), como NDVI, SAVI, GNDVI e NDRE. Estes índices são calculados automaticamente numa aplicação intuitiva, permitindo aos agricultores analisar o crescimento das plantas, identificar condições de stress e tomar decisões de gestão informadas.

A validação experimental, realizada com um conjunto de imagens multiespectrais de acesso público, demonstrou a capacidade da plataforma de identificar variações no vigor das culturas e no teor de clorofila ao longo de diferentes fases de crescimento. Os resultados destacam a relevância do uso de imagens multiespectrais como uma ferramenta fiável, sem contacto e económica para práticas agrícolas sustentáveis.

De modo geral, esta investigação promove a transformação digital na agricultura, oferecendo uma plataforma de apoio fácil de usar que aumenta a produtividade das culturas e incentiva o uso eficiente dos recursos.

Palavras-Chave: Agricultura de Precisão, Imagens Multiespectrais, Índices de Vegetação, Veículo Aéreo Não Tripulado, Monitorização de Cultivos, Processamento de Imagens

Abstract

The growing challenges of food demand, climate variability, and resource scarcity have highlighted the need for innovative technological solutions in agriculture. This work presents a software platform for the analysis of multispectral images of agricultural fields for Precision Agriculture, with a focus on improving crop monitoring and resource management.

The proposed platform integrates data collected from Unmanned Aerial Vehicles (UAVs) equipped with multispectral sensors to assess vegetation health using spectral vegetation indices (VIs), such as NDVI, SAVI, GNDVI, and NDRE. These indices are computed automatically within a user-friendly desktop application, allowing farmers to analyse plant growth, identify stress conditions, and make informed management decisions.

Experimental validation employing a publicly available multispectral dataset demonstrated the platform's capacity to identify variations in crop vigour and chlorophyll content across various growth stages. The results highlight the relevance of multispectral imaging as a dependable, non-destructive, and cost-efficient instrument for sustainable agricultural practices.

Overall, this research advances the digital transformation of agriculture by providing a user-friendly decision-support platform that enhances crop productivity and encourages the efficient utilisation of resources.

Keywords: Precision Agriculture, Multispectral Imaging, Vegetation Indices (VIs), Unmanned Aerial Vehicle (UAV), Crop Monitoring, Image Processing

Contents

List of Tables

List of Figures

List of Acronyms

COG - Cloud Optimised GeoTIFF

DSRM - Design Science Research Methodology

GNDVI - Green Normalised Difference Vegetation Index

IoT - Internet of Things

ML - Machine Learning

NDRE - Normalised Difference Red Edge Index

NDVI - Normalised Difference Vegetation Index

NIR - Near-Infrared

PA - Precision Agriculture

PRISMA - Preferred Reporting Items for Systematic Reviews and Meta-Analyses

RGB - Red, Green and Blue

SAVI - Soil-Adjusted Vegetation Index

SVI - Spectral Vegetation Index

UAV - Unmanned Aerial Vehicle

VI - Vegetation Index

CHAPTER 1

Introduction

1.1 Background and Motivation

The Internet of Things (IoT), despite seeming to be a recent topic, was first used in 1999 by Kevin Ashton, a British technology pioneer. He used it to describe a system where, through sensors, objects from our daily lives could be connected to the Internet [1]. These devices can now be referred to as “smart” devices and their emergence has transformed today’s industries, enhanced daily living, and redefined human interactions with the surrounding environment.

Nowadays, IoT is no longer a distant dream but the reality of our lives. It has contributed to the economic growth, sustainability and increased efficiency in various areas, such as retail, infrastructure, transportation, healthcare, energy, environment and agriculture [2], which are the focus of this research.

Despite being one of the greatest sources of food in the world, agriculture still faces many problems due to the world’s current state. In 1800, the world’s population reached its first billion, 130 years later, its second, 30 years later its third, by 2011, it was already at 7 billion, and, by 2050, it is expected to exceed 9.7 billion [3]. As a result, the global climate has changed, causing significant fluctuations in the environment’s temperature, affecting not only people’s well-being but also the crops as well [4]. t has also resulted in water scarcity, as less freshwater is available for irrigation, which is essential for crop growth and is required in large quantities [5]. Another consequence of global population growth is the need for urban expansion, which has led to a further reduction in available arable land, as only 55% of ice-free land is currently used for agriculture [6].

Over the years, agricultural efficiency has increased steadily; however, due to these factors, it is still insufficient, leading to a greater use of fertilisers and pesticides to address this problem [7]. However, this will eventually lead to a shortage of resources, and, combining that with most farmers' low budget, such resources become something not to be wasted.

Several parameters influence crop health, including temperature, water availability, soil nutrients, the presence of pests and weeds, chlorophyll content in plants, and weather conditions [8]. The application of new technologies in agriculture, known as Precision Agriculture (PA),

focuses on the acquisition and analysis of data related to these parameters. This enables farmers to identify which parameters are required to maintain crop health, as well as those that may cause crop stress or deterioration, and to understand where, when, and in what quantities they are needed. Thus, PA can help to reduce the waste of these resources by indicating when, where, and how much is needed, helping farmers to reduce their expenditure on them.

To address these challenges, researchers have proposed the use of imagery to accelerate issue identification. The most commonly used types include RGB, thermal, multispectral, and hyperspectral imagery, which can be captured via UAVs, aircraft, or satellites. This topic will be explored in greater detail later in Chapter 2.

This thesis aims to develop a tool for processing and analysing multispectral images, transforming them into actionable insights to support farmers in monitoring and improving crop health

1.2 Research Questions

The questions below emphasise the main elements that direct the analysis in this research:

- How can multispectral imaging improve the accuracy and scope of agricultural monitoring?
- Which key vegetation indices and metrics can be derived from multispectral image data, and how do they reflect crop conditions?
- How do spatial filtering techniques influence the accuracy of vegetation index–based crop assessments?
- What potential environmental and economic benefits can result from adopting multispectral imaging technologies in agriculture?
- How can user interface design enhance the accessibility and adoption of multispectral image analysis tools by farmers?

1.3 Objectives

The main objective of this thesis is to develop a system capable of processing and analysing multispectral imagery obtained via an Unmanned Aerial Vehicle (UAV). The platform was designed to assess crop development and vegetation health through the computation of various

vegetation indices (VI). To accomplish this objective, the project was divided into two main goals.

The initial objective was to establish a comprehensive image analysis workflow capable of efficiently managing multispectral data. This includes facilitating the upload, processing, and visualisation of multispectral images, as well as integrating automated computation of essential VI.

The second objective was to design and develop an intuitive and interactive platform interface that enables users to perform analyses at various levels. This approach aims to provide flexibility in examining vegetation conditions across different spatial contexts, thereby aligning the system with the practical needs of PA.

1.4 Research Method

The research method chosen to address this dissertation was the Design Science Research Methodology (DSRM). Its iterative nature makes DSRM ideal for this research, as it enables continuous refinement of the system by revisiting previous stages whenever complications arise, ultimately leading to the best possible solution [9].

This method consists of six different stages. On the first stage, its intent is to identify the problem this work has chosen to focus on: the waste of limited agricultural resources and farmer's poor economic situation. The second phase is about defining the objectives to be achieved with this work. These can be found in the objectives chapter of this study. The next stage focusses on the design and development of the prototype proposed in this thesis. Firstly, the problem is analysed, and, with the help of a literature review, the best possible hardware and software was chosen in order to design the ideal prototype to fight the problem that is the subject of this work. Finally, the prototype was developed according to the previously made choices. Then, comes the testing and evaluation stages, where the prototype will go under evaluation through an extensive series of tests, to find any possible errors or possible improvements. If the prototype does not fully meet the established requirements, earlier methodological phases are revisited to refine the system's design based on evaluation outcomes. After going through all these stages, and cycle through them, until the best possible outcome has been achieved, the last and final stage of this research method follows: the communication

stage. In this stage, the outcomes of the study are formally documented and disseminated. These stages are represented in Figure 1.1.

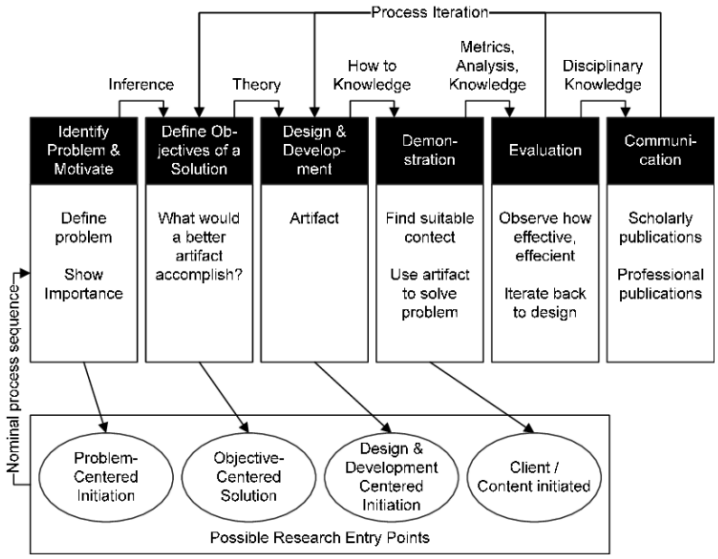

Figure 1.1 - Design Science Research Methodology [9]

1.5 Thesis Structure

This thesis is structured as follows:

- Chapter 1 (Introduction) – This section starts by introducing the subject under study and giving some context about its background and motivation for its study. To provide clear direction, the research questions and objectives are then presented. And finally, the research method and thesis structure.
- Chapter 2 (Literature Review) – This chapter presents some understanding of the concepts discussed in this work, as well as information on previous work that may improve the one done in this thesis.
- Chapter 3 (Vegetation Indices) – This chapter explains the theoretical foundations and mathematical formulations of the vegetation indices used in this study. Each index is examined in terms of its principles, uses, and limitations.
- Chapter 4 (Software) – This section describes the development of the designed platform. It covers the system's architecture, key functionalities, and user interface.
- Chapter 5 (Results and Discussion) – This chapter presents and discusses the findings derived from the analysis of multispectral images. The evaluation is conducted at three distinct levels, with comparative analyses performed to assess the system's performance and reliability.

- Chapter 6 (Conclusion and Future Work) – The final chapter summarises the principal findings and contributions of the study. It additionally delineates the primary limitations faced during the project and proposes future improvements.

CHAPTER 2

Literature Review

2.1 Systematic Review

For this research, multiple studies were analysed in order to establish the background context. The article databases utilised included Scopus, Google Scholar, IEEE Xplore, MDPI and Elsevier. To obtain relevant results, a search was conducted based on some keywords, such as “Multispectral Images”, “Precision Agriculture”, “Machine Learning”, “Remote Sensing”, “Image Processing” and “Plant Disease Detection”. Since not all results were directly relevant, a filtering process was applied, restricting the selection to articles available for free or within ISCTE’s scientific license, written in English, and from the year 2014 to 2025. To obtain the papers with relevant information for this study, the PRISMA (Preferred Reporting Items for Systematic Reviews and Meta-Analyses) methodology was used.

Initially, 889 papers were obtained based on the combination of keywords and the specified criteria. Then the duplicates were removed, resulting in a total of 434 articles. Subsequently, the abstracts were reviewed, and 328 articles were excluded, leaving 106 articles for analysis. A thorough examination of these articles was conducted, ultimately selecting 31 for inclusion in the study. The flowchart of the research is represented in Figure 2.1.

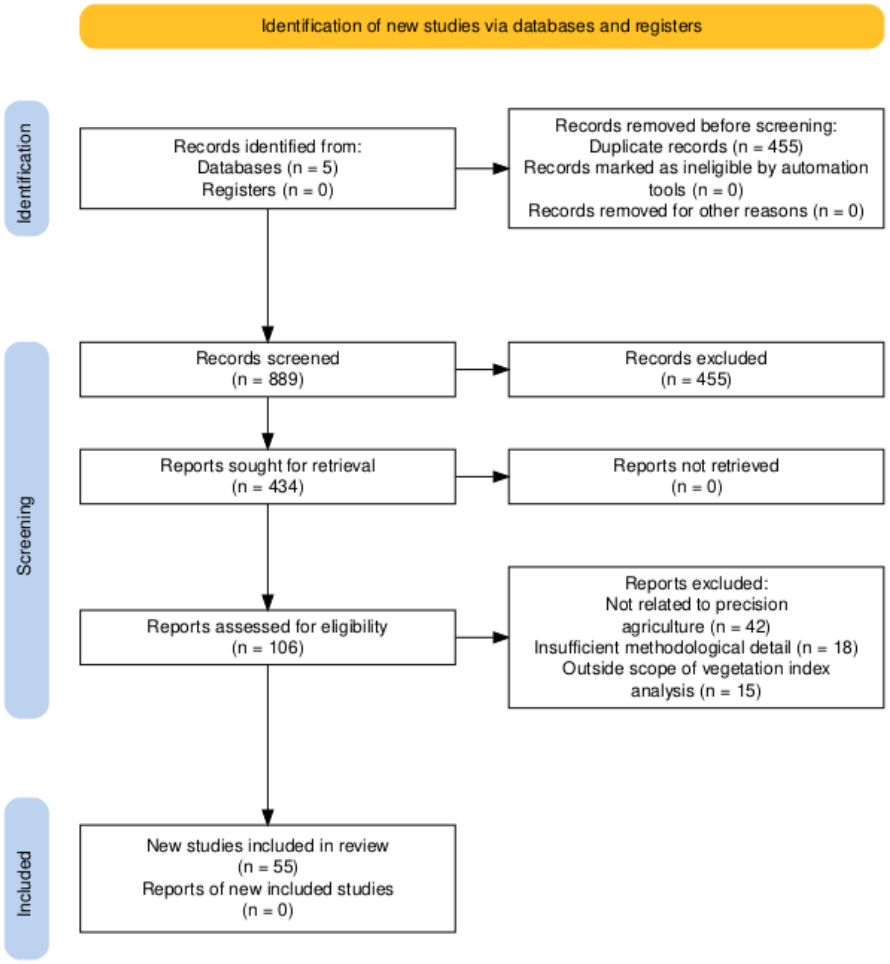

Figure 2.1 - Systematic Review Flowchart

2.2 Related Works

This chapter will provide an overview of existing studies relevant to this research. Topics like the various applications of IoT in PA, various sensing techniques employed in farming, types of imagery used in agriculture, along with their optimal applications, will be addressed in order to establish some essential background for the study.

2.2.1 Internet of Things Applications in Precision Agriculture

By integrating IoT into agriculture, farmers are able to overcome a great number of challenges, such as resource management, climate change, and food security, among others. With the help of IoT technologies such as smart sensors, real-time analytics, and automated irrigation systems, farmers can monitor crop conditions, optimise water management, regulate chemical application, and even detect the presence of diseases in their fields.

These applications, therefore, not only increase the efficiency of agriculture but also contribute to a more sustainable food system for future generations.

2.2.1.1 Smart Monitoring

One IoT application in PA is Smart Monitoring, which enables farmers to collect real-time data, such as soil conditions, environmental changes, crop health, and more. By collecting and analysing this data, farmers can make accurate decisions to improve crop yields and overall farm management.

For instance, M. Mondal et al. [10] developed an IoT-based intelligent agriculture field monitoring system. His goal was to enable farmers to make informed decisions regarding irrigation schedules and crop management, thereby optimising water usage and improving overall crop yield. He focused on monitoring various environmental parameters such as soil moisture and temperature, which have the greatest impact on irrigation needs and crop growth.

Similarly, S. Tenzin et al. [11] also aimed to enhance crop management and sustainable agricultural practices. However, he instead developed a weather monitoring system. With it, he not only could monitor the soil moisture and temperature, but also relative humidity, wind speed and direction, precipitation and light.

Moreover, A. Triantafyllou et al. [12] proposed an architectural model for a smart farming monitoring system in which he combined the use of sensors with thermal cameras on UAVs. With the sensors, he could monitor moisture content, temperature, humidity, soil chemical properties and environmental parameters such as wind speed and solar radiation. With the thermal cameras, he would instead monitor soil and vegetation characteristics, such as colour, chlorophyll content and overall crop health. The combination of these two technologies could significantly improve plant production and growth.

2.2.1.2 Smart Irrigation

With the support of IoT technologies such as weather forecasting services, soil moisture sensors, and automated irrigation systems, farmers can determine the amount of water required by crops and the optimal timing for irrigation. In practice, Smart Irrigation solutions are typically implemented through dedicated software platforms or decision support systems that

integrate sensor data stored in local or cloud-based databases, together with external data sources such as meteorological services.

A. D. Boursianis et al. [13] and S. Roy et al. [14] were two of many authors who worked on this topic. Both developed a smart irrigation system where, based on the monitored data, they could schedule an irrigation for when their crops needed it most. Their intent was to optimise the farmer's water usage, thereby reducing water wastage and improving irrigation efficiency.

Similarly, A. Al-Naji et al. [15] developed a smart irrigation system to enhance water efficiency. However, instead of monitoring soil conditions, he came up with the idea of using RGB cameras to monitor soil colour variations. He then used this data to train an artificial neural network, thereby being able to tell more accurately whether irrigation was needed or not.

2.2.1.3 Smart Fertilisation

Smart Fertilisation is conceptually similar to Smart Irrigation, with both employing automated systems tailored to irrigation and fertilisation. This IoT application enables optimised fertiliser management, leading to lower chemical inputs and reduced environmental impact.

An example of this technology is presented by M. Badreldeen et al. [16]. In their work, soil conditions were monitored to support informed decisions regarding the timing and spatial distribution of fertilisation, enabling automated system adjustments and the selection of appropriate fertiliser types according to crop nutrient requirements at different growth stages. This approach reduces chemical inputs and improves resource utilisation.

Rather than automating fertiliser application, J. Sun et al. [17] focused on reducing human involvement in the monitoring and decision-making processes associated with fertilisation. Their approach involved monitoring soil nutrient levels, such as nitrogen (N), phosphorus (P), and potassium (K). These parameters were classified into predefined levels, and when any value fell below an acceptable threshold, the system automatically notified the user via email, indicating the need for fertilisation and recommending the appropriate fertiliser type.

2.2.1.4 Disease Detection

Diseases and pests cause massive yield losses, on average 17.2 % for potatoes, 21.4% for soybeans, 21.5% for wheat, 22.6% for maize and 30.3% for rice, making them one of the most impactful factors in yield losses. For this reason, researchers have begun to develop tools in order to fight this problem and increase food security [18].

For instance, S. Ghosal et al. [19] developed a deep machine vision framework. This framework utilised ML techniques in RGB images to identify, classify and quantify bacterial and fungal diseases, chemical injuries, and nutrient deficiencies. By doing so, crop productivity and plant breeding could improve significantly. L. C. Ngugi et al. [20] also used ML techniques, more specifically, convolutional neural networks (CNNs), in RGB images collected from mobile phones to detect leaf diseases.

Similarly, J. Su et al. [21] monitored yellow rust disease in wheat using unmanned aerial vehicles (UAVs) equipped with multispectral cameras. He was later able to extract the spectral characteristics and the Spectral Vegetation Indices (SVIs) from the recorded images and thus distinguish the healthy from the diseased plants more precisely. A. di Nisio et al. [22] and M. Kerkech et al. [23] also utilised UAVs equipped with multispectral cameras along with image processing techniques, except that A. di Nisio used this technology to detect Xylella fastidiosa in olive trees and M. Kerkech used it to identify diseased areas in vineyards.

In addition, S. Cubero et al. [24] developed a robotic platform capable of detecting and monitoring pathogens in horticultural crops, more precisely, a disease known as CaLsol. In this work, the robot he developed used not only RGB images but also hyperspectral ones, enabling a more detailed analysis of the plant's health.

J. S. Duhan et al. [25], unlike the other authors, utilised a different technology from ML in images. Despite his purpose being the same as the others, he used nanomaterials, such as quantum dots and nanoparticles, as biosensors to detect pathogenic organisms associated with the various existing plant diseases.

2.2.2 Sensing in Agriculture

Ever since ancient times, when it was first created, agriculture has come a long way. One of the causes for that evolution were the sensors. Before being used in this field, all tasks had to be

done by humans. Today, with the help of sensors, many of these tasks have become automated and those that were not, at least no longer require as much effort as before.

This technology can be categorised into two different types: in-situ sensing and remote sensing.

2.2.2.1 In-situ Sensing

In-situ sensing consists of the act of detecting and monitoring the desired parameters directly on site, which guarantees an almost immediate response time. With this approach, data such as soil temperature, moisture and nutrient levels can be measured to make informed decisions regarding the irrigation or fertilisation needs, as mentioned before.

For example, X. Pei et al. [26] utilised a multi-sensor named Veris P4000 to collect visible and near-infrared spectral data, electrical conductivity, cone index readings and depth information regarding soil properties. His goal was to estimate multiple soil profile properties using in-situ sensor data acquired.

N. Nair et al. [27], also used an in-situ sensing approach in his work. Since conventional methods of measuring soil pH are time-consuming and require sophisticated instruments and a skilled operator, he developed an all-solid electrode, in-situ soil pH sensor in order to mitigate these setbacks.

Although both studies achieved their respective objectives, limitations associated with the in-situ sensing approach were identified. In particular, variations in soil properties, such as structure, moisture content, and temperature, were observed to significantly influence measurement accuracy.

2.2.2.2 Remote Sensing

Remote sensing consists of the act of measuring the physical characteristics of an area, but instead of being right at its source, like in-situ sensing, this approach occurs far away from its source. This method is mostly implemented with the help of three types of platforms: satellite, aircraft or UAV.

Each of these platforms has its limitations and advantages. A. Matese et al. [28], conducted a study with that goal in mind. He compared the use of these three platforms in precision viticulture and analysed both the economic and operational pros and cons of the platforms. Table 2.1 shows the technical specifications of the three platforms analysed in his work.

Table 2.1 - Platform's Technical Specifications [28]

	UAV	Aircraft	Satellite
Platform	Mikrokopter OktoXL	Sky Arrow 650 TC/P68	RapidEye
Camera	 Tetracam ADC Lite	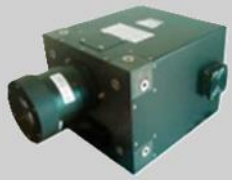 ASPIS	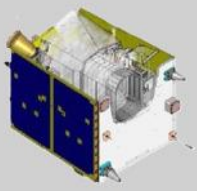 REIS
Number of channels	3	12	5
Dimension	114 x 77 x 22 mm	270 x 250 x 200 mm	656 x 361 x 824 mm
Weight	0.2 kg	10 kg	62 kg
Output data	10 bit RAW	8 bit RAW	16 bit NITF
Image Size	6 MB	4 MB	462 MB/25 km along track for 5 bands
Flight quote AGL	150 m	2300 m	630 km
Ground resolution	0.05 m/pixel	0.5 m/pixel	5 m/pixel
Ground image dimension	116.5 x 87.5 m	1024 x 1024 m	77 x 45 km
Total frames	100	2	1

In operational terms, the study concluded that satellite platforms offer superior range, reliability, payload capacity, and mosaicking and geocoding capabilities, whereas UAVs perform less effectively in these aspects. Conversely, UAVs provide greater flexibility, higher spatial resolution, faster processing, and lower dependence on cloud cover, while satellite platforms are less effective in these characteristics. Regarding endurance and processing time, both aircraft and satellite platforms were found to be superior to UAVs. These comparisons are summarised in Table 2.2.

Table 2.2 - Platform's characteristics (++optimal, + good, o average, - poor) [28]

Characteristics	UAV	Aircraft	Satellite
Range	-	+	++
Flexibility	++	+	-
Endurance	-	++	++
Cloud cover dependency	++	+	-
Reliability	o	+	++
Payload	o	+	++
Resolution	++	+	o
Precision	++	+	o
Mosaicking and geocoding effort	-	o	++
Processing time	o	+	+

Looking at Figure 2.2 from an economic perspective, it can be seen that the cost per area increases for all platforms, with the exception of the satellite, whose cost per area is always the same. UAVs are initially the most cost-effective option, however, as the surveyed area increases, they eventually become the most expensive. The Aircraft, just like in operational terms, remains the better-balanced option between all three platforms.

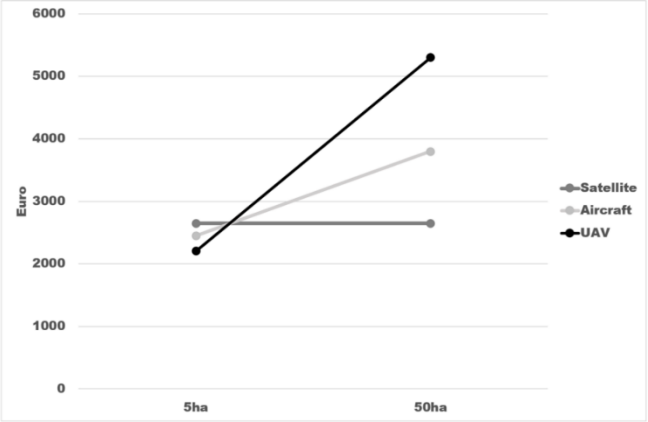

Figure 2.2 - Platform's costs [28]

Although UAV platforms typically exhibit limited range and endurance, the objective of this work is to analyse plant- and leaf-level characteristics, for which high spatial resolution and image precision are essential. UAV-based imagery is therefore particularly well suited to this purpose, as it offers superior resolution, operational flexibility, and reduced dependence on cloud coverage when compared to alternative platforms.

From an economic perspective, UAV operations tend to become more costly as the surveyed area increases; however, the spatial scale relevant to this study does not exceed 5 hectares. Consequently, UAVs remain an appropriate reference platform for this type of analysis.

For these reasons, and in line with several related studies [12, 21–23], this work adopts multispectral imagery acquired using UAV platforms. Due to practical constraints, the analysis is conducted using a publicly available UAV-based dataset rather than imagery collected directly within this study.

2.2.3 Applied Imagery in Precision Agriculture

One of the most innovative technological approaches in agriculture is the use of applied imaging technologies. Through platforms such as satellites, aircraft, and UAVs equipped with cameras and sensors, it is possible to capture detailed images of crops and soil, enabling the assessment of plant health, optimisation of water and fertiliser use, and early detection of diseases before they spread.

Since UAVs are the platform that is going to be used in this study, they will also be analysed. In order to use applied imagery through UAVs, they need to be equipped with certain types of cameras, which usually are: RGB, thermal, multispectral and hyperspectral.

2.2.3.1 Types of Imagery

Each type of cameras captures images with different characteristics. RGB cameras record in the visible wavelength range of the spectrum and are therefore unable to acquire health-related information [29]. Thermal cameras convert the radiation emitted from the surface of an object into temperature, making them more suitable for temperature stress-related measurements [30]. Multispectral cameras can capture in the red, green, blue and near-infrared (NIR) bands of the electromagnetic spectrum, which is very useful in agriculture since the NIR is highly reflected by the vegetation [31]. In general, hyperspectral cameras are similar to multispectral ones, the only difference being the hyperspectral ability to capture in a wider range of bands [32].

R. Guebsi et al. [33] and N. Delavarpour et al. [34] both conducted a study where their goal was to analyse the different applications of each type of imagery used in UAVs. They concluded that for RGB cameras, crop monitoring, health assessment, vegetation analysis and indexing, 3D mapping and structural analysis were the most common applications. Thermal cameras excel in water stress and irrigation management, as well as in vegetation and thermal analysis. For multispectral cameras, crop health and stress monitoring, VIs, and nutrient analysis were this camera's speciality. Lastly, hyperspectral cameras were highly proficient in plant

identification, biochemical and nutritional analysis, and soil and vegetation analysis. These conclusions are described in Table 2.3.

Table 2.3 - Camera's common applications [33-34]

Camera Type	Common Applications
RGB	Crop monitoring
	Health assessment
	Vegetation analysis and indexing
	3D mapping
	Structural analysis
Thermal	Water stress and irrigation management
	Vegetation and thermal analysis
Multispectral	Crop health and stress monitoring
	Vegetation indices and nutrient analysis
Hyperspectral	Plant identification
	Biochemical and nutritional analysis
	Soil and vegetation analysis

As previously mentioned, the aim of this work is to monitor crop health and stress. Thus, the type of camera and, consequently, imagery to be used is multispectral, as it best suits this study's objectives.

CHAPTER 3

Vegetation Indices

As mentioned before, multispectral images take a big role in precision agriculture and crop monitoring. They are able to do so because of the radiance values extracted from the various wavebands captured by the multispectral cameras. They can capture the normal RGB image and in five bands: Blue, Green, Red, RedEdge, and Near-Infrared (NIR), as shown in Figure 3.1. The values extracted are usually collected simultaneously and reflect the vegetation state from which they were acquired. By combining these values, researchers are capable of creating vegetation indices (VI) [35].

Figure 3.1 – DJI Phantom 4 multispectral camera [36]

These formulae play a vital role in precision agriculture and crop monitoring, since they offer a cost-effective, contactless and simple yet reliable way of crop monitoring, providing an accessible and environmentally sustainable means of assessing crop health and condition. Depending on the selected VI, different insights can be obtained regarding plant growth and development. Some give information about the leaf area, others about the chlorophyll content of the crop, there are some that provide data about the canopy structure and some even about water status [37]. Different vegetation indices are suited to different analytical purposes: some are applicable to a wide range of objectives, while others are designed for more specific assessments. And since they demonstrate different sensitivities, making them more appropriate

for specific stages of the crop growth cycle, some have a better performance on the early stages of the plant's growth, and others on the later stages [38]. If used correctly, the information obtained from the VIs can then be utilised to optimise fertiliser and pesticide application, and irrigation, in other words, precision agriculture.

3.1 Normalised Difference Vegetation Index

The Normalised Difference Vegetation Index, or NDVI, is, historically, the most widely used VI due to its simplicity and robustness.

This index combines the red and near-infrared (NIR) reflectance in order to exhibit leaf anatomy and chlorophyll content. The following equation represents it:

$$NDVI = \frac{NIR - Red}{NIR + Red} \quad (1)$$

NDVI can range from -1 to +1, as water sources usually correspond to negative values, values close to zero correspond to bare soils, and positive values to vegetation [35, 39]. Since it depends greatly on the spectral behaviour of green vegetation, where the chlorophyll absorbs radiation in the red region of the electromagnetic spectrum and the leaf structures reflect radiation in the near-infrared region of the spectrum, areas with elevated vegetative productivity are categorised by lower red and higher near-infrared reflectance [40].

NDVI values are greatly related to key biophysical parameters, such as leaf area index, vegetation percentage cover, green biomass, and overall plant health and vigour. It can be used to evaluate vegetation activity temporarily and spatially, allowing the detection and determination of environmental disturbances such as fire, flood, drought, and frost [41]. From an agricultural perspective, it is capable of providing significant insights about food security and ecosystem productivity, because of the plant stress, photosynthetic capacity, and agricultural crop yield assessment features [37].

Despite being the most used VI, NDVI also has its own limitations. For instance, aspects like sensor calibration differences, atmospheric conditions such as scattering and haze, and directional reflectance effects related to sun-sensor geometry, make its values vary significantly [39]. Another disadvantage consists of the fact that the topographic relief can further influence the reflectance measurements, once the background effects are problematic when vegetation cover is scarce, since soil reflectance greatly contributes to the overall canopy signal, making

darker soils more prone to increase NDVI values, and consequently making it biased in vegetation assessments [42]. Lastly, NDVI shows saturation in dense vegetation cover, where chlorophyll content or biomass increases no longer mean proportional increases in the index [39].

3.2 Soil-Adjusted Vegetation Index

The Soil-Adjusted Vegetation Index (SAVI) was first introduced by Huete et al. [43] as an improvement to the NDVI, designed to decrease the influence of soil background reflectance on vegetation monitoring, particularly in sparsely vegetated environments. SAVI integrates a soil-adjustment factor, represented by L, which accounts for the proportion of vegetation cover within a scene. This index is expressed by the following equation:

$$SAVI = \frac{NIR - Red}{NIR + Red + L} \times (1 + L) \quad (2)$$

NIR and Red correspond to near-infrared and red reflectances, respectively, and L can range from 0 to 1 depending on the vegetation density. When vegetation cover is complete, L approaches zero, and SAVI becomes equal to NDVI. On the other hand, in sparsely vegetated areas, larger L values are used in order to mitigate soil brightness [43].

SAVI has been widely applied in ecological and agricultural studies where soil visibility strongly makes a difference in vegetation assessments. SAVI has also proven effective in mapping rangeland and dryland vegetation, where indices like NDVI tend to miscalculate greenness due to soil background effects [43-44]. Additionally, this index is also frequently used for land degradation, desertification, and ecological restoration efforts assessment, offering better sensitivity to variations in green vegetation under circumstances of low canopy density [45]. By reducing the soil background reflectance influence, SAVI provides more reliable information on vegetation dynamics in environments where NDVI is less accurate.

Despite its improvements over NDVI, SAVI still has its own limitations. A crucial constraint lies in the selection of the L factor, as a fixed value provides only a pragmatic compromise and may not be optimal across different vegetation densities or soil backgrounds [46-47]. SAVI's accuracy also depends on the soil line parameters, with deviations in slope or intercept reducing its reliability [47]. Similar to NDVI, SAVI also suffers from saturation at dense vegetation cover sites, where further increases in vegetation biomass or chlorophyll content are no longer captured proportionally. Moreover, the index also does not correct for

atmospheric effects such as scattering or for bidirectional reflectance effects caused by illumination variations and viewing geometry. Its accuracy also differs depending on soil type, illumination conditions, and sensor spectral characteristics, which limit its universality [43, 46-47].

3.3 Green Normalised Difference Vegetation Index

The Green Normalised Difference Vegetation Index (GNDVI) is a variation of the usual NDVI that replaces the green spectral band for the red band with the purpose of enhancing sensitivity to chlorophyll content and mitigating index saturation under high vegetation cover [48]. It is represented by the following equation:

$$GNDVI = \frac{NIR - Green}{NIR + Green} \tag{3}$$

NIR represents near-infrared reflectance, and Green represents the green reflectance. The foundation for GNDVI lies in the fact that healthy vegetation, which is abundant in chlorophyll, reflects strongly in the green region and weakly in the red. Consequently, GNDVI has a stronger linear correlation with chlorophyll concentration, leaf area index, nitrogen content, and overall biomass when compared to NDVI [49].

GNDVI, due to its enhanced sensitivity to chlorophyll and nitrogen content, has been strongly used in agricultural, ecological, and remote sensing studies. In precision agriculture, it is commonly used to monitor crop nitrogen status, track chlorophyll concentration, and assess vegetation vigour, more specifically during the mid to late growth stages when NDVI often saturates [48]. Outside agriculture, GNDVI is also used for leaf area index estimation, biomass accumulation, and the proportion of photosynthetically absorbed radiation. Some studies comparing GNDVI with NDVI have shown that GNDVI can offer similar spatial patterns to NDVI while providing greater discernment in dense vegetation cover conditions, making it useful in applications such as rangeland monitoring, habitat condition assessment, and ecological restoration projects [50].

GNDVI, like all indices, also has its own limitations that constrain its applicability. As a two-band index, it remains sensitive to atmospheric effects, adjacency influences, and shadowing, which can cause variability unrelated to vegetation properties. As already mentioned, although it saturates more slowly than NDVI, GNDVI may still have saturation in vegetation-dense crops, limiting its effectiveness in highly productive ecosystems.

Additionally, its dependence on the green band increases vulnerability to scattering effects, soil background contributions, and understorey vegetation signals, which may influence canopy reflectance estimates in heterogeneous landscapes [48-49].

3.4 Normalised Difference Red Edge Index

The Normalised Difference Red Edge Index (NDRE) was invented to enhance sensitivity to leaf chlorophyll and nitrogen content, particularly under conditions where NDVI tends to saturate [51]. This index is expressed by the following equation:

$$NDRE = \frac{NIR - RedEdge}{NIR + RedEdge} \quad (4)$$

NIR refers to near-infrared reflectance, and RedEdge to the reflectance in the red-edge portion of the spectrum. Unlike GNDVI, which uses the green band, NDRE employs the red-edge band that pierces deeper into the leaf, making it more effective for assessing chlorophyll in dense vegetation [51-53]. Therefore, NDRE is best suited for mid to late stages of crop growth, when chlorophyll content is high and NDVI becomes less responsive [51-53]. The values of this index can range from -1 to 1, with higher values reflecting greater chlorophyll and nitrogen concentration [54].

NDRE has become widely applied in crop nitrogen management, offering information about canopy nitrogen dynamics and supporting more accurate fertiliser recommendations, mostly during mid to late growth stages [53-54]. NDRE has also been successfully used to perceive nitrogen-limited areas in crops such as wheat, corn, soybeans, and tree seedlings, allowing early intervention in order to optimise plant nutrition and yield [53-54]. And just like NDVI, NDRE is also used in ecosystem and vegetation assessments, where its capability to detect variations in chlorophyll and canopy structure offers more reliable data on plant vigour and stress conditions [54].

Regarding its limitations, NDRE is also sensitive to atmospheric effects, sensor calibration, and illumination conditions [54]. And although it reduces saturation relative to NDVI, it can still be less responsive under great vegetation cover or high biomass conditions, where reflectance variations in the red-edge and near-infrared regions are lessened [54]. Just like GNDVI, this index may also be influenced by leaf structure, shadows, soil background, or mixed pixels, which can introduce noise in heterogeneous landscapes [54]. Lastly, the

effectiveness of NDRE is strongly growth stage-dependent, making it less accurate at early growth stages when chlorophyll content is relatively low [53].

CHAPTER 4

System Software

This chapter describes the desktop application created and its backend and frontend functionalities. This application was developed with the purpose of giving farmers a platform to upload their own multispectral images and analyse them according to the indices they select. It was designed with a focus on user experience (UX), explicitly addressing the needs of farmers and their difficulties in identifying the necessities of their crops. This approach allows for faster and more targeted decision-making, which can, in turn, contribute to a continuous increase in crop productivity and a decrease in resource waste.

4.1 System Architecture Tools

To create this platform, three key tools were used: Python for backend development, Electron and React for the frontend, and SQLite for the database. Together, these tools form the foundation of the system and define its overall architecture. The following sections provide a detailed description of each tool and its role within the platform.

4.1.1 Python

Python is one of the most used programming languages in scientific research, data analysis, and software development. Its simple interface and wide standard library make it an easy tool that is able to support both rapid prototyping and large-scale applications. During the development phase, a preliminary assessment of several programming languages was conducted to determine the most suitable option for this platform. Python was ultimately chosen because it provides a balanced combination of simplicity, flexibility, and a comprehensive ecosystem of libraries that support efficient data processing and integration with analytical processes, while its strong community support and broad range of specialised packages further enhance its capabilities, especially in areas like numerical computation, image processing, and machine learning. In this project, Python was employed for backend development, serving as the main language responsible for handling data processing, image processing and system logic.

4.1.2 Electron and React

Electron is a framework that allows developers to build cross-platform desktop applications using web technologies, such as HTML, CSS, and JavaScript. This framework, combined with React, a component-based JavaScript library for building user interfaces, makes it possible to create desktop applications which are as visually responsive as functionally reliable. This approach allows the use of just one codebase to run on different operating systems, such as Windows, macOS, and Linux, while maintaining consistent performance and design. In this project, Electron and React were used to develop the frontend of the platform, offering an intuitive interface through which farmers can upload multispectral images and analyse them.

4.1.3 SQLite

SQLite is a small, fast, self-contained, highly reliable, full-featured, serverless, relational database management system widely used in desktop and mobile applications. In contrast to server-based databases, SQLite stores data in a single file, making it easy to integrate into applications without requiring a separate database server or internet access. It can withstand standard SQL queries, transactions, and indexing, therefore providing reliable data storage and retrieval. In this project, SQLite was used as the database for the platform, managing the storage of multispectral images.

4.2 Database Creation

As mentioned before, SQLite was chosen as the database engine for this project. It was chosen primarily because of its serverless architecture, since one of the goals of this thesis was to provide farmers with a platform capable of analysing multispectral images in real time, and since internet access cannot always be guaranteed in agricultural settings, a serverless database was the most appropriate choice.

This database was designed based on the type of information farmers are likely to require in real-life analyses. To address these needs, a set of objects was created to support the storage, organisation, and processing of multispectral image data. These objects include tables for essential entities, junction tables to manage the relationships between the objects, and default entries to enable VI calculations immediately after initialisation.

4.2.1 Objects

The main object of this project is the ImageDTO, which represents the multispectral image selected by the user for analysis. This object stores the image name, the timestamp indicating when it was captured, and an optional description field that allows users to record comments for later reference. In addition, it maintains references to the spectral bands available in the image, the farm to which the image belongs, and the plant types contained within it. The code used to create the ImageDTO table in the database is represented in Figure 4.1.

```
# Create ImageDTO table
cursor.execute("""
    CREATE TABLE IF NOT EXISTS ImageDTO (
        id INTEGER PRIMARY KEY AUTOINCREMENT,
        name TEXT NOT NULL,
        capturedAt TEXT,
        bandsId INTEGER,
        description TEXT,
        farmId INTEGER,
        plantId INTEGER
    )
""")
```

Figure 4.1 - ImageDTO creation code

Considering the need for structured data organisation, the FolderDTO object was designed to allow users to flexibly group and organise images. A folder can contain multiple ImageDTO objects or even other FolderDTO objects, thereby building a hierarchical structure. Similar to ImageDTO, this object also includes fields for name and description, as well as references to the farm and plant types associated with its contents. A crucial feature of this object is that updates to these references are automatically propagated to its children, ensuring data consistency across the whole hierarchy.

To manage the spectral band information associated with each image, the BandsDTO object was created. The visible field stores the path to the JPEG file of the image, while the cog field stores the path to the Cloud Optimised GeoTIFF (COG) file, which consolidates all spectral bands into a single file. The remaining fields (blue, green, red, redEdge, and NIR) are used to specify the availability of each band, where a value of 1 indicates that the band is available and 0 indicates that it is unavailable.

Finally, to complement the information stored in images and folders, the FarmDTO and PlantDTO objects were created. Each object contains a single field, name, whose purpose is to serve as its identifier. What differs in these two is their purpose: FarmDTO is used to track farms, while PlantDTO is used to track plant types.

Lastly, to support the image analysis, VegetationIndicesDTO object was created. This object stores the formula of each VI, enabling the platform to process the reflectance values of images correctly. Additionally, it stores the index name for easier identification and a description to inform the user about the purpose and calculation of each index. All the objects mentioned are described in Table 4.1.

Table 4.1 – Database created objects and corresponding descriptions

Objects	Description
ImageDTO	Represents a multispectral image
FolderDTO	Organises and groups images or other folders hierarchically
BandsDTO	Stores the spectral band information for each image
FarmDTO	Represents a farm entity to which images or folders can be associated
PlantDTO	Represents a plant type contained in the images or folders
VegetationIndicesDTO	Stores vegetation index formulas, names, and descriptions

4.2.2 Structure

After the objects were defined, attention was given to the overall structure and relationships between them. The database was designed to reflect the real-world associations among images, folders, farms, and plant types. One-to-many and many-to-many relationships were implemented using foreign keys and junction tables to keep data integrity and support complex queries.

To support the hierarchical structure that was wanted for folders, the parentFolderId field was add to the FolderDTO object. This field is a foreign key referencing the ID of another folder in the same table, allowing a folder to contain multiple child folders while maintaining a link to its parent folder. To enable folders to also store images, the junction table named FolderImages was created. This table allows a one-to-many relationship between FolderDTO and ImageDTO.

To track the relationship between plants and images or folders, the ImagePlants and FolderPlants junction tables were created, supporting many-to-many associations. Each record in these tables links a single ImageDTO or FolderDTO entry to a specific PlantDTO, allowing

a single image or folder to reference multiple plant types and, on the other hand, a single plant type to be associated with multiple images or folders. Just as FolderImages, these tables also ensure that each reference is valid through foreign key constraints, while cascading updates and deletions maintain consistency across the database.

Similarly, to track the relationship between images or folders and farms, junction tables for ImageFarms and FolderFarms were created. Each record in these tables links a single ImageDTO or FolderDTO entry to a specific FarmDTO, establishing a one-to-many relationship: a single image or folder can reference only one farm, while a single farm can be associated with multiple images or folders.

At last, to manage the spectral bands required by each VI, the VegetationIndexBands junction table was created. This table establishes a many-to-many relationship between the VegetationIndicesDTO, and the corresponding spectral bands used in their formulas. Each record specifies the index identifier, the band name, and its positional order within the formula.

Figure 4.2 displays the complete database schema, showing the objects, their main attributes, and the relationships established between them.

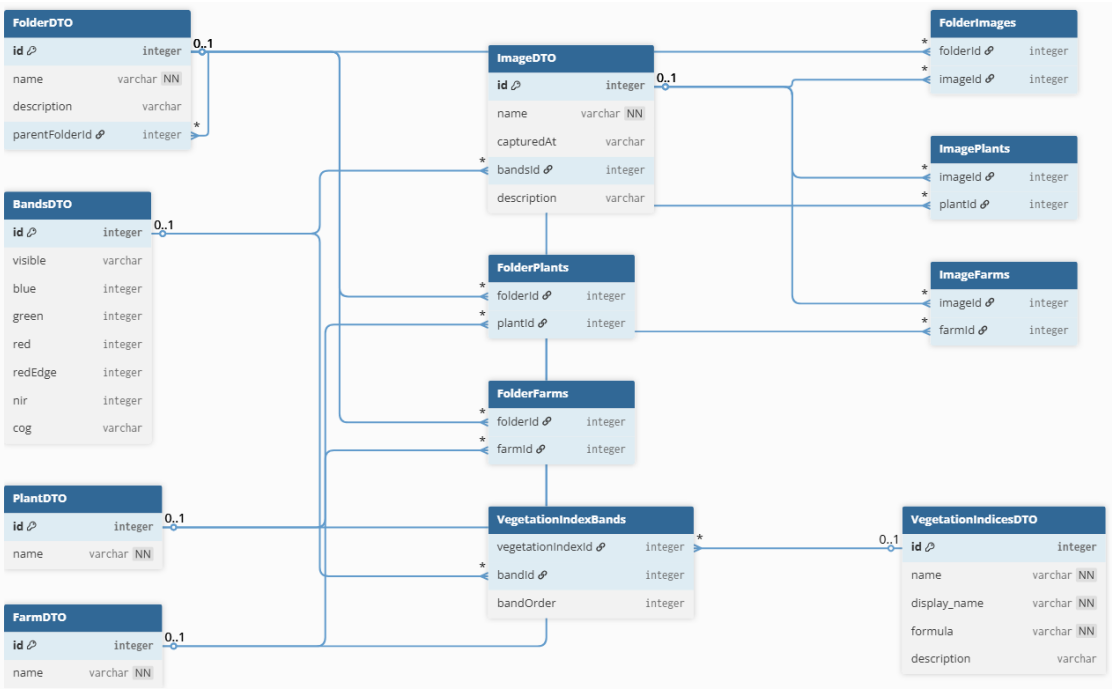

Figure 4.2 – Database Model

4.3 Design and Functionalities

This application was designed with one goal in mind: to provide farmers with an intuitive and efficient tool for analysing multispectral images. During its development, several aspects were carefully considered to ensure that the final product would be both easy to use and accessible in environments without internet connectivity. The platform integrates data organisation, visualisation, and analytical capabilities within a user-friendly interface, allowing users to easily navigate between image organisation, VI calculation, and result analysis. This section presents the main functionalities of the application alongside its interface design and the overall flow of user interaction through the platform.

4.3.1 Functionalities and Interface

One of the main functionalities of the application is its ability to easily upload and manage multispectral images directly from local storage. The interface for this feature was designed to make the process as straightforward as possible, allowing users to import images or folders in supported formats. During this process, the system automatically generates a COG file containing the available bands and stores all related metadata in the local SQLite database. The user has the ability to choose between uploading a single image or an entire folder. In the case of a single-image upload, the user may be unaware of the spectral band to which the image corresponds. In that case, the platform will automatically perform this process, identify it, and create an ImageDTO object. Suppose the user chooses to upload a whole folder. In that case, the platform performs a recursive analysis, creating a FolderDTO object for the selected directory and for each nested subfolder that exists within it. It also groups the related .tif and .jpeg files and generates an ImageDTO object for each group. The image/folder upload modal is represented in Figure 4.3.

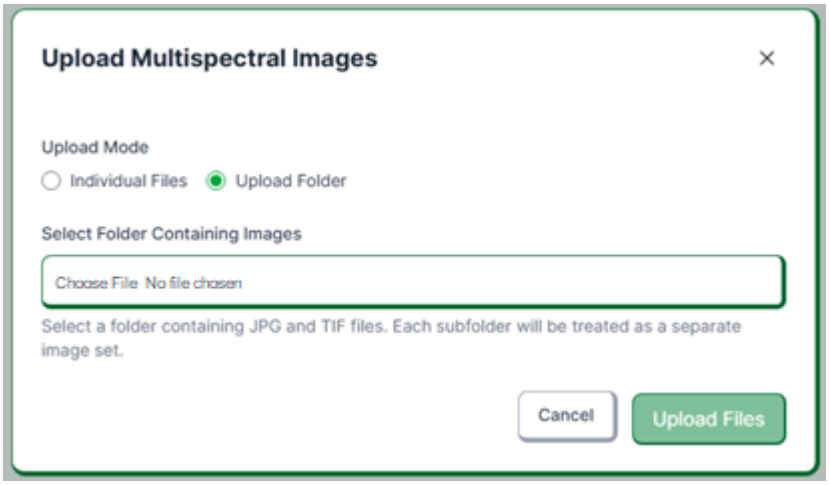

Figure 4.3 – Upload Multispectral Images Modal

Moving on to the home screen, since the entire platform was designed with ease of use in mind, this page was no exception. Therefore, it was decided to use a design that most people were familiar with, being similar to the appearance of most computer desktops. Here is where the entire data organisation will take place, as shown in Figure 4.4.

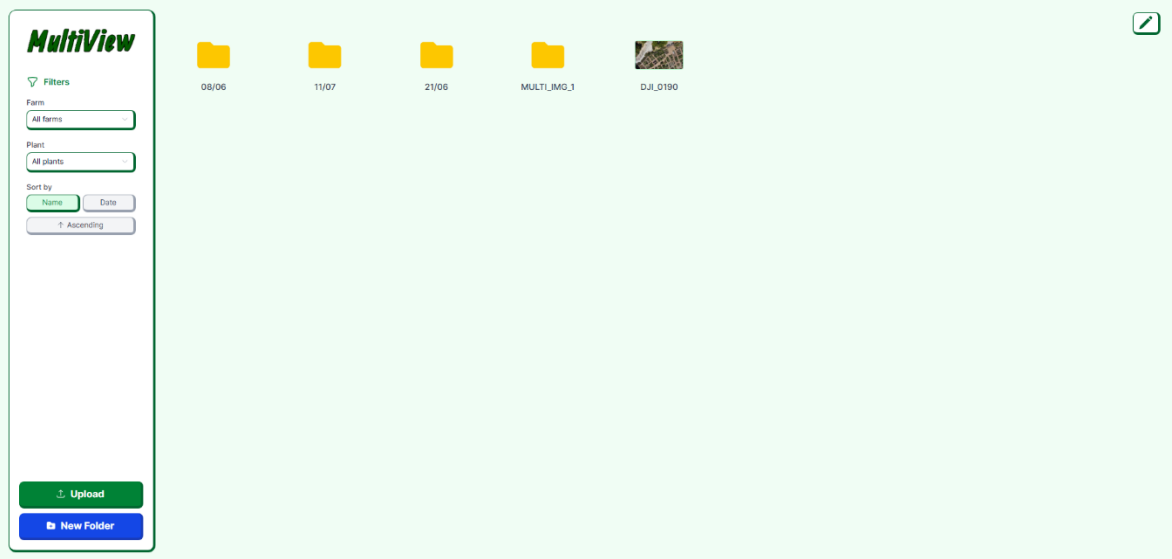

Figure 4.4 – Platform's data organization page

By clicking on the button with the pencil icon in the top right corner, the user enters edit mode. There, he is capable of organising the FolderDTO and ImageDTO objects as he wants by dragging one into the other, similar to how it is done on a computer desktop. He can also right-click on the folder or image objects, and a small menu will open, as shown in Figure 4.5.

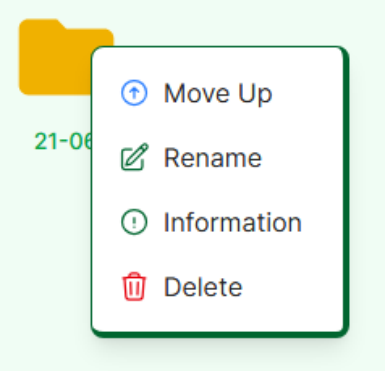

Figure 4.5 – Folder's options menu

It contains three or four options, it always includes the "Rename", "Information", and "Delete" options, and the "Move Up" option appears if the object is not located at the root of the storage. By clicking on that option, that object will move one place up on the path. The

"Rename" option allows the user, as the name suggests, to rename the object. "Delete" will delete the object recursively, including all objects contained within it, if it is an instance of FolderDTO. "Information" option opens the modal shown in Figure 4.6.

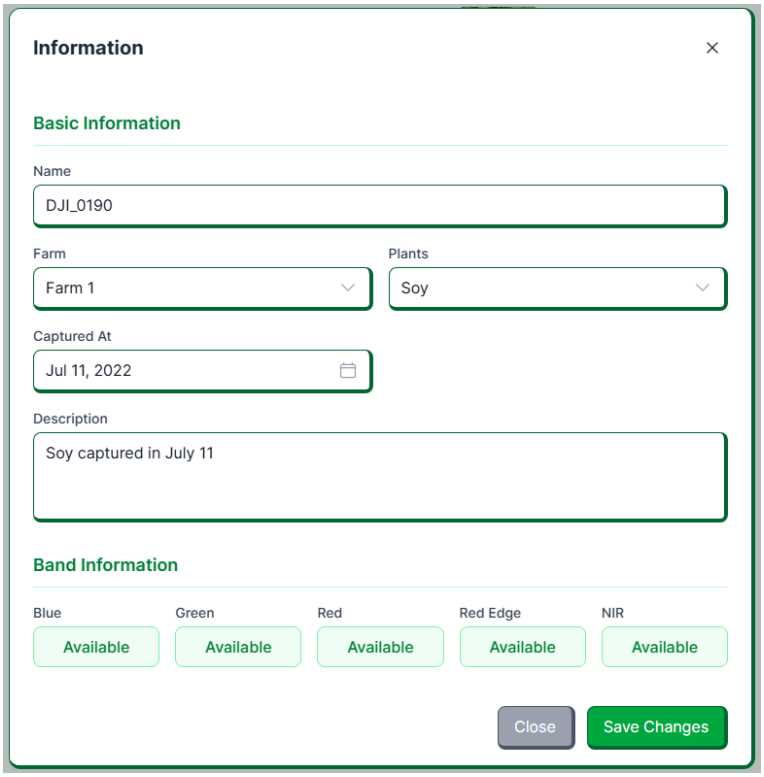

Figure 4.6 – Information Modal

This modal is divided into two sections: "Basic Information," which is common in both folder and image objects, and "Band Information", which only appears in image objects. In the first section, the user can edit the object's info. There, he can rename it, associate the farm to where the object belongs, associate the different plant types that the object contains, select a date so he knows when the image was taken, and add a description in case he wants to leave any comments about it. The "Band Information" section is for informational purposes, providing details on which bands are available.

Looking back at Figure 4.4, on the left side of the home page, a sidebar is available. There, the user is provided with two buttons: one to create a new folder object and the other to open the upload modal, along with some filters. Through these options, the user can filter the displayed objects by farm or plant and also sort the objects alphabetically or chronologically, in either ascending or descending order.

Moving on to another platform functionality, when the user left clicks on an image object, the platform opens the image analysis page, as illustrated in Figure 4.7.

Figure 4.7 – Platform's image analysis page

As shown in Figure 4.7, the page initially displays the .jpeg file associated with the selected ImageDTO object. On the right side of the interface, the user is presented with six buttons: the first returns to the home page, the second opens the information modal shown in Figure 4.6, the third activates selection mode, allowing the user to choose a specific area of the image, and the remaining three buttons let the user zoom in or out as desired and reset the image to its original state. On the left side of the interface, similarly to the previous page, there is also a sidebar. It starts by providing the user with four default indices to choose from for analysis, where they can also find a button with a plus icon that opens the modal shown in Figure 4.8.

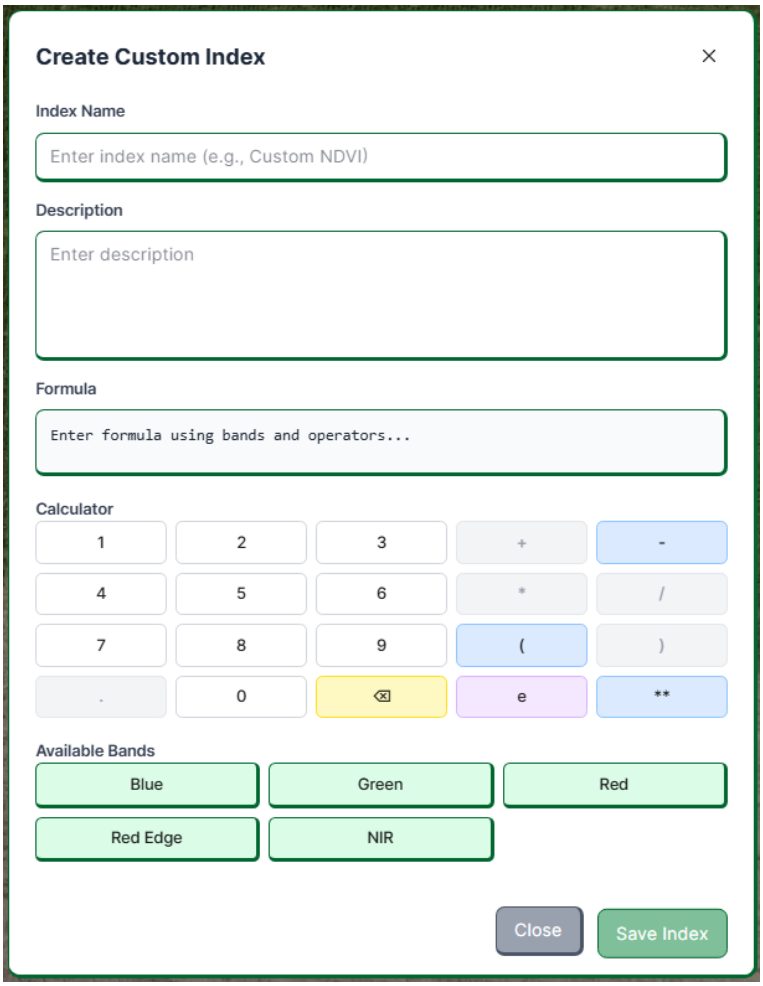

Figure 4.8 – Create Custom Index Modal

Here, the user can add an index of its choice. The first two inputs allow the user to define the index's name and description. Below, they write the equation associated with the index using the embedded calculator and band buttons.

Returning to the analysis page, when the user selects one of the already defined indices or one that they add themselves, the platform will process the image using the associated equation and calculate the corresponding value for every pixel, resulting in something similar to what is represented in Figure 4.9.

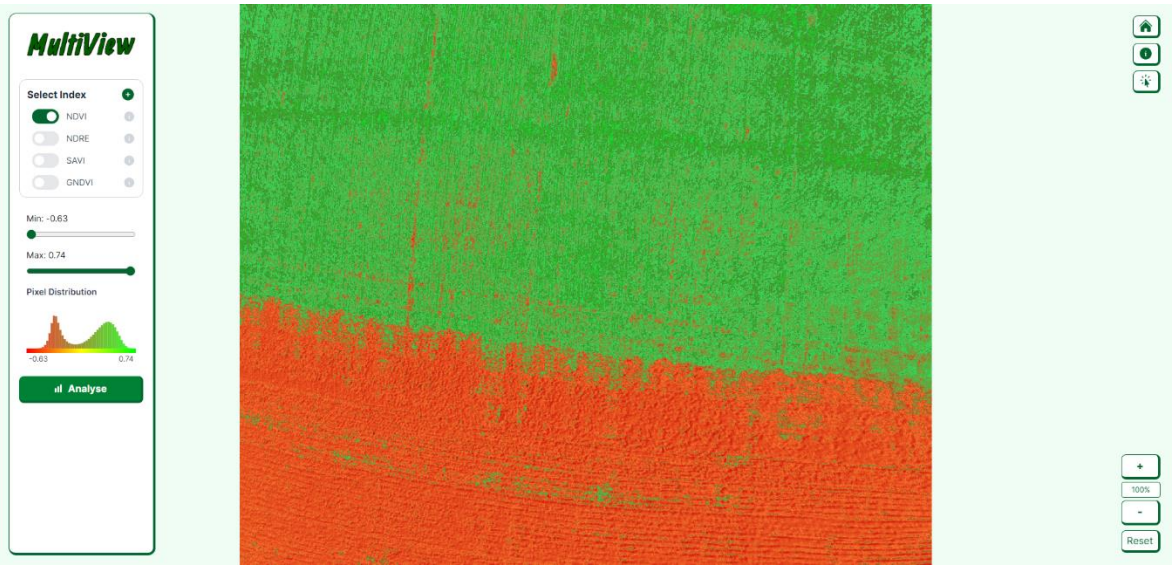

Figure 4.9 – Platform's analysis page with NDVI index selected

After calculating each pixel's value, the app paints them using a gradient from red to green, where red represents the minimum value calculated and green represents the highest, usually corresponding to unhealthy and healthy vegetation, respectively. Note that, if the user has selected a specific area, the platform will only paint that area, as shown in Figure 4.10.

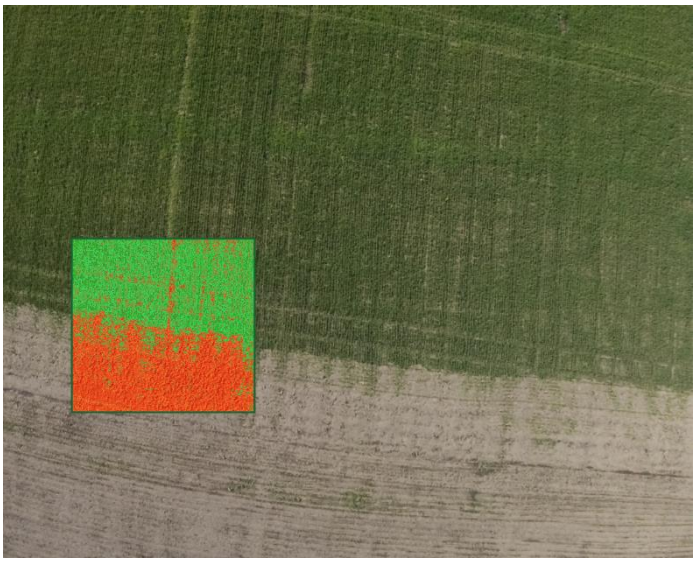

Figure 4.10 – Specific area analysis

After selecting a VI, additional features become available in the sidebar. The first of these is two sliders that set the minimum and maximum values of the calculated index, as displayed in Figure 4.11 a). By adjusting them, users can specify the value range to display. For example, setting the minimum to 0 and the maximum to 0.75 will display only those pixels with values

within that range, as shown in Figure 4.11 b). This helps users concentrate on specific VI value ranges that are most relevant to their analysis. Another feature, designed to assist users in interpreting results, includes a histogram that displays the pixel value distribution over the area, highlighting the most predominant values, also shown in Figure 4.11 a).

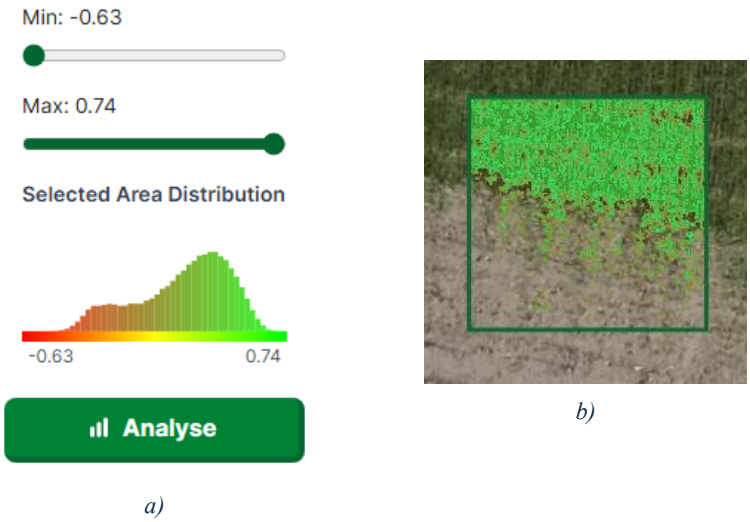

a) *b)*

Figure 4.11 – a) Min and max sliders and pixel histogram; b) Specific area analysis with min slider set to 0 and max slider set to 0.74

Additionally, clicking the analysis button opens a modal showing the mean index value of the area. When a default index is selected, the modal provides a brief interpretation of the result, the healthy percentage area, and guidance on how the farmer should proceed to treat the analysed area based on the area's health assessment, the healthy percentage, and the chosen index. To help the farmer know the exact location of the analysed area, it also shows the area's coordinates obtained from the multispectral images' metadata. For instance, selecting NDVI might indicate whether the area has healthy or stressed vegetation, as illustrated in Figure 4.12. All these functionalities work in both the whole image and in a specific selected area.

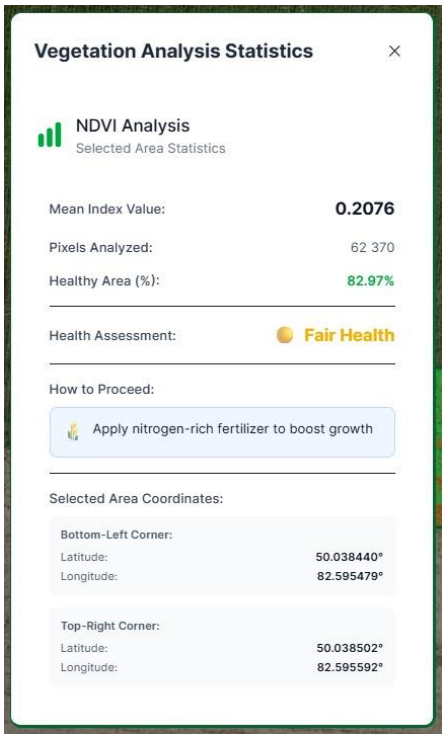

Figure 4.12 – Vegetation Analysis Statistics Modal

4.3.2 User Flow

In order to have a simple and intuitive user-system interaction, the application features a clear and logical workflow that reflects the natural order of image analysis steps.

The interaction starts on the home page, where the user begins to upload new multispectral images or folders from local storage. After importing the desired images, they are automatically processed and saved in the database, keeping the same organisation that they had when uploading.

Once they are uploaded, the user can navigate through the created folders and images and select one for analysis. Having chosen one, the application opens the analysis page, where the user can visualise the corresponding .jpeg image and select the index they want to use for analysis. Here, he can also adjust value ranges through maximum and minimum sliders, visualise histograms of pixel distributions, and evaluate mean index values or system-generated assessments.

After an analysis is completed, the workflow may be repeated for additional images. Previously uploaded data persist within the platform across multiple executions, enabling successive analyses without the need for data re-import. This process is illustrated in Figure 4.13.

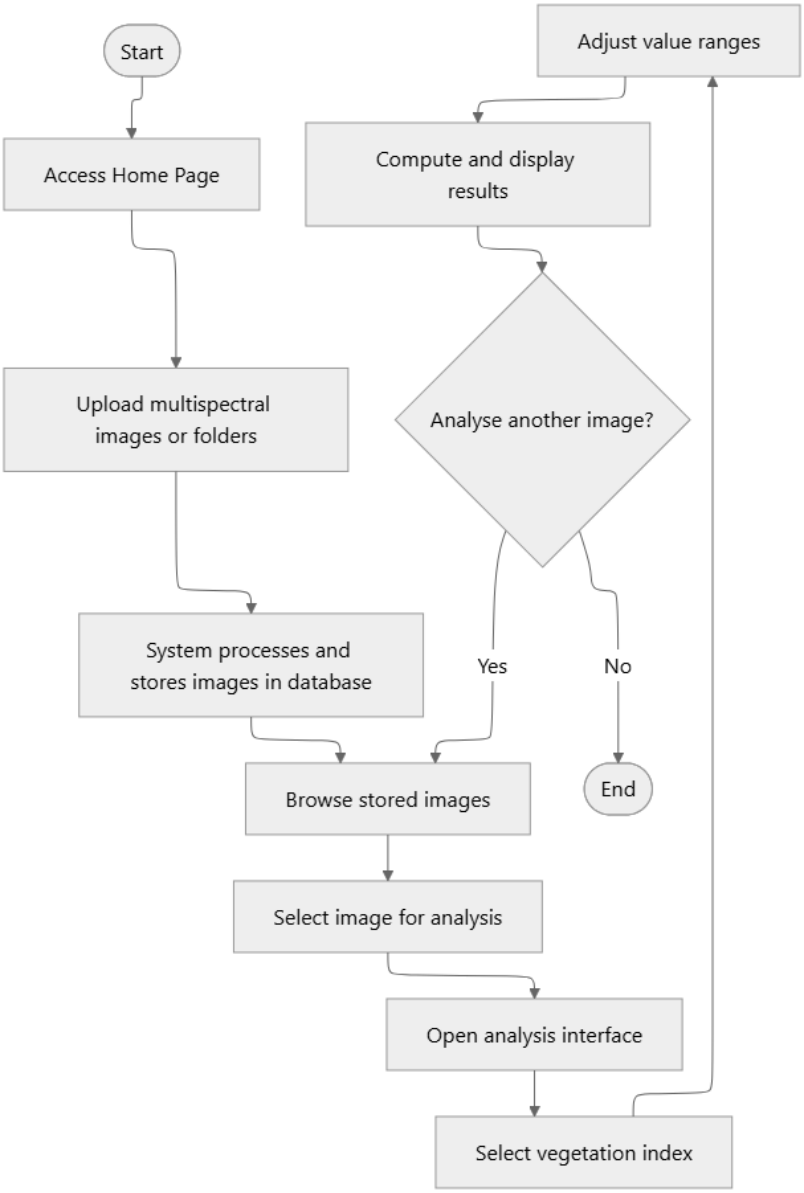

Figure 4.13 – User Flowchart

CHAPTER 5

Results and Discussion

This section presents the results obtained through the analysis of multispectral images using the developed platform. The main goal of this analysis is to assess the accuracy and utility of the platform's analytical features in real-life agricultural scenarios, alongside evaluating how various VIs behave throughout the different plant growth stages.

To start this analysis, a collection of multispectral images was necessary. Due to limited access to drones with the required capabilities, the decision was made to utilise a public dataset. The dataset used in this study was obtained from an article authored by Maulit et al. (2023) [55], which offers multispectral drone imagery collected in the East Kazakhstan region of the Republic of Kazakhstan, near the city of Ust-Kamenogorsk, at coordinates 50º02' N 82º35' E. This dataset was chosen due to its completeness and diversity, as it includes images captured at various crop growth stages and from different crop types, thereby facilitating a dependable evaluation of the platform.

This dataset covers an area of 27 hectares, cultivated with wheat, barley, and soybean at various stages of their growth, utilising a DJI Phantom 4 multispectral UAV equipped with a 6 × 1.29-inch CMOS multispectral camera. It consolidates images from five aerial multispectral photography sessions conducted on 17 and 18 May 2022, 8 and 9 June 2022, 21 and 22 June 2022, 11 and 12 July 2022, and 25 and 26 July 2022. During each session, substantial efforts were made to ensure consistent weather conditions, characterised by clear sky coverage, captured at approximately the same time with closely matched temperature, sun elevation, azimuth angle, and wind speed.

For this study, the sessions selected for analysis were the ones conducted on 8 and 9 June 2022, 21 and 22 June 2022, and 11 and 12 July 2022, as these dates most accurately represented the various stages of crop growth, namely early to mid, mid, and mid to late stages, respectively. The earliest and latest sessions available within the dataset were excluded, as these corresponded to periods when the plants were either too young or too old, thereby making them less suitable for vegetation development analysis.

5.1 Image Analysis

To achieve the objective of this chapter, an analysis of a specific area across the three growth stages was conducted at three distinct levels: initially, the entire images were examined; subsequently, a specific area was analysed; and finally, an analysis of a particular masked area was performed. The VIs introduced in the Indices chapter were used throughout all analyses to assess crop development and vegetation health.

5.1.1 Image Analysis Over the Entire Area

The evaluation started by analysing the entirety of the image for each selected date. This step was taken in order to provide a general idea of vegetation vigour throughout the different crop growth stages using the VIs implemented in the platform and introduced previously, namely NDVI, SAVI, GNDVI, and NDRE. Through these indices, it was possible to obtain an assessment of plant health, canopy structure, and chlorophyll content.

Figures 5.1-5.3 display the generated index maps for the three analysed dates (8 June, 21 June, and 11 July 2022) corresponding to the early to late growth stages. Each one of the index's maps was generated by the platform, using the corresponding multispectral image bands. Areas indicated in green represent regions of higher vegetation vigour. In contrast, orange or red tones correspond to zones of lower vegetation vigour or areas of bare soil or senescent vegetation.

Analysing the images from Figure 5.1, it is possible to observe that in all four indices, a substantial area of green tones is already present in the upper half of the images. Nevertheless, some still exhibit visible regions of orange and red tones, indicating bare soil or very early crop development. This pattern aligns with the expected conditions during the initial growth stage.

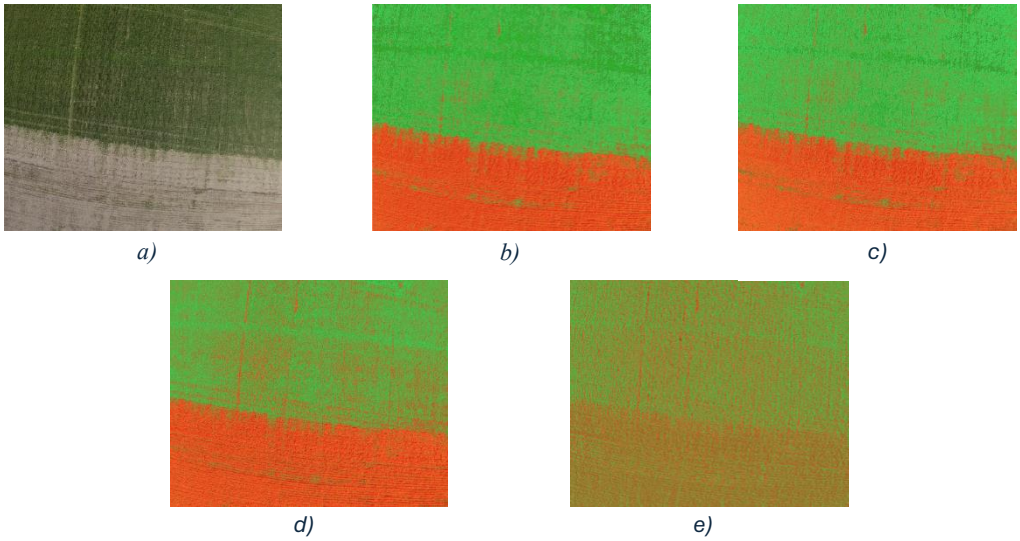

Figure 5.1 – JPEG image and index maps for 8 June from whole image analysis; a) JPEG image; b) NDVI; c) SAVI; d) GNDVI; e) NDRE

At this stage, the differences between the upper and lower halves of the images are still evident, as shown in Figure 5.2. The upper half continues to display mainly green tones, whereas the lower half mainly displays red tones. In comparison with the previous stage, there has been a reduction in the orange and red regions across all indices. The NDVI and SAVI maps show these tones have almost completely vanished, indicating a more vigorous canopy. Although some orange and red areas persist in the GNDVI and NDRE maps, their diminution signifies an increase in chlorophyll content. This suggests that most of the field has progressed to a more advanced vegetative state, with only a few isolated zones of bare soil or low chlorophyll activity remaining.

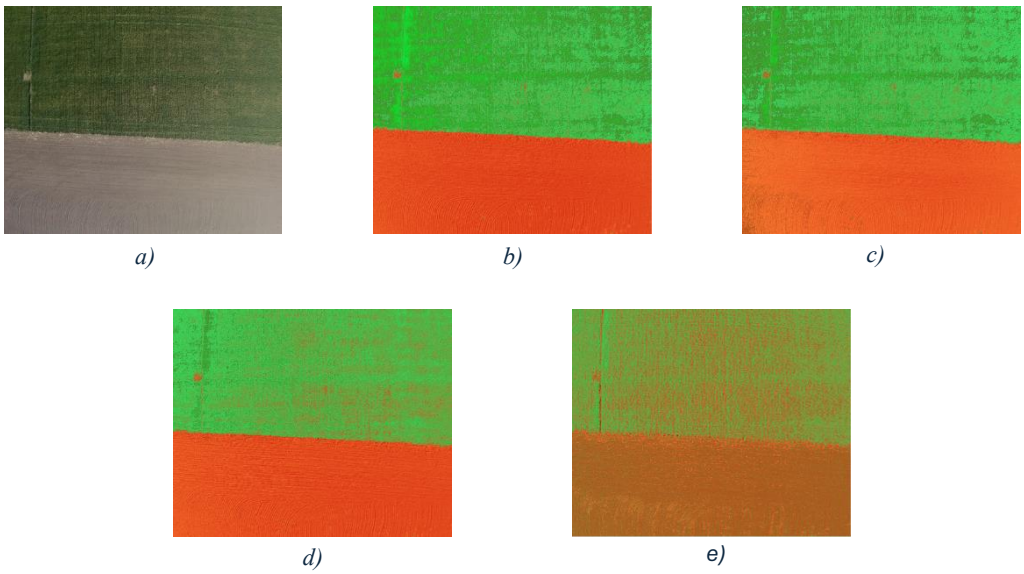

Figure 5.2 – JPEG image and index maps for 21 June from whole image analysis; a) JPEG image; b) NDVI; c) SAVI; d) GNDVI; e) NDRE

In the final stage, a general decline in vegetation vigour is observed across all indices, closely resembling the initial stage, as displayed in Figure 5.3. The NDVI and SAVI maps, which previously showed highly green dense areas, now display reduced green areas and increased red tones. The NDRE and GNDVI indices similarly demonstrate lower overall values, indicating a decline in chlorophyll content. This behaviour aligns with the anticipated growth stage of the crops at this point in the season.

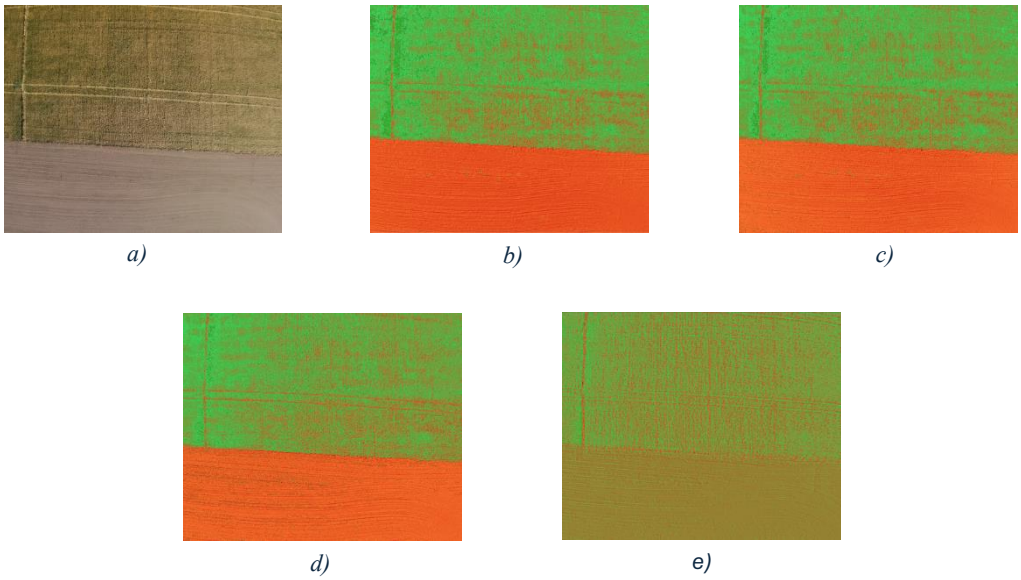

Figure 5.3 – JPEG image and index maps for 11 July from whole image analysis; a) JPEG image; b) NDVI; c) SAVI; d) GNDVI; e) NDRE

Table 5.1 presents the mean values computed by the platform for each VI for the whole image analysis, along with the qualitative assessment generated based on predefined thresholds.

The qualitative assessments associated with each vegetation index are derived from predefined threshold intervals applied to the mean index values. These thresholds were defined within the platform to provide an intuitive interpretation of vegetation condition, reflecting commonly accepted ranges reported in the literature. For NDVI and SAVI, the intervals represent overall vegetation health, ranging from “Very Poor Health” at values below 0.1 to “Excellent Health” at values equal to or above 0.6. GNDVI and NDRE thresholds are instead oriented toward chlorophyll content, with lower or negative values indicating non-vegetated or low-chlorophyll areas and higher values corresponding to increased chlorophyll concentration.

Table 5.1 – Whole image analysis results

Indices		Date		
		08/06/2022	21/06/2022	11/07/2022
NDVI	Mean	0.1197	0.0979	0.0104
	Analysis	Poor	Very Poor	Very Poor
SAVI	Mean	0.0417	0.0374	0.0050
	Analysis	Very Poor	Very Poor	Very Poor
GNDVI	Mean	-0.0142	-0.0411	0.0086
	Analysis	Non-Vegetated	Non-Vegetated	Low
NDRE	Mean	-0.0311	-0.0448	-0.0039
	Analysis	Very Low	Very Low	Very Low

Analysing the table, it can be seen that all indices present relatively low mean values. NDVI and SAVI show a decline from 0.1197 and 0.0417 on 8 July 2022 to 0.0104 and 0.0050 on 11 July 2022, respectively. This decline suggests a reduction in the field's overall vigour. Similarly, GNDVI and NDRE exhibit near-zero or negative values across all dates, corresponding to "Non-Vegetated", "Very Low" or "Low" assessments by the platform.

These results demonstrate that, although the platform effectively captures the overall temporal progress of vegetation conditions, the presence of non-crop areas, such as soil paths and roads, significantly impacts the mean values, thereby lowering the overall assessments.

5.1.2 Image Analysis of a Specific Area

To mitigate the influence of non-crop areas, an identical assessment was conducted on a designated region of the image. This evaluation followed the same methodology, applying the NDVI, SAVI, GNDVI, and NDRE indices to the designated area for each examined date.

Figures 5.4-5.6 present the index maps generated for the three examined dates (8 June, 21 June, and 11 July 2022), corresponding to the early to late growth stages.

At this stage, different from the whole image analysis, green tones are much more abundant than red ones across most indices, as represented in Figure 5.4. This observation indicates that the selected area predominantly corresponds to actively vegetated regions. The decreased presence of red tones in the NDVI, SAVI, and GNDVI indices suggests limited bare soil or non-vegetated zones, which aligns with early-stage crop development, as previously indicated. Nevertheless, in the NDRE map, several regions exhibiting red tones remain visible, implying

that the crops have not yet reached full maturity and that chlorophyll concentration remains relatively low. This behaviour corresponds with NDRE's heightened sensitivity to subtle variations in leaf structure and chlorophyll content, thereby reducing its performance during early growth stages.

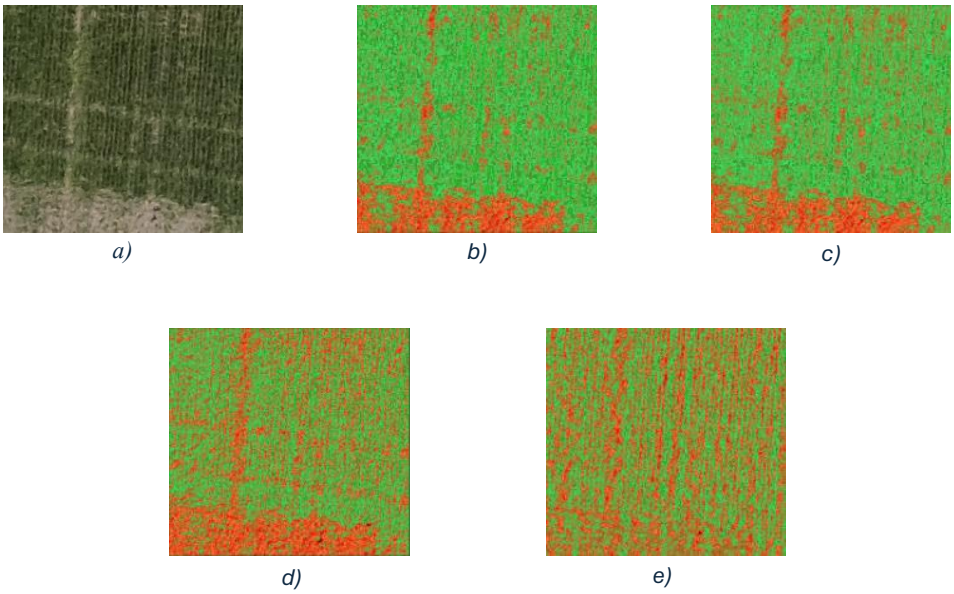

Figure 5.4 – JPEG image and index maps for 8 June from specific area analysis; a) JPEG image; b) NDVI; c) SAVI; d) GNDVI; e) NDRE

Similar to the second date in the whole image analysis, this stage also demonstrates an increase in green-toned areas and the disappearance of most red zones within the vegetated regions, as displayed in Figure 5.5. NDVI and SAVI maps display red-toned zones exclusively where bare soil is present, whereas GNDVI and NDRE continue to exhibit some red zones within the vegetated areas. Compared to the previous date, NDRE shows an increase in green-toned regions, reflecting its higher sensitivity to chlorophyll content and confirming its enhanced performance during later stages of crop development.

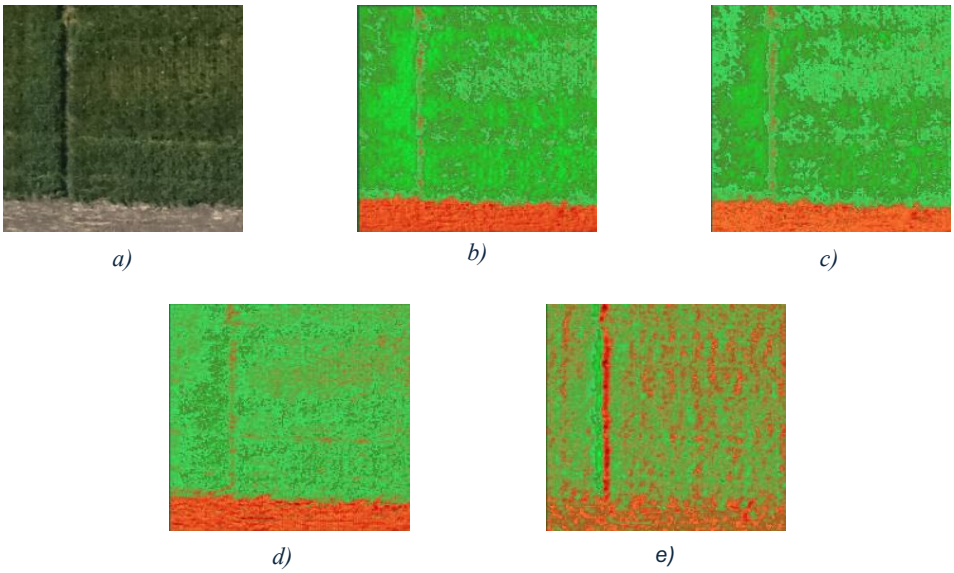

Figure 5.5 – JPEG image and index maps for 21 June from specific area analysis; a) JPEG image; b) NDVI; c) SAVI; d) GNDVI; e) NDRE

At this stage, the NDVI, SAVE, and GNDVI maps once again show the return of the red-toned zones within the vegetated area, indicating a decrease in vegetation vigour as the crops reach the end of their development, as shown in Figure 5.6. In contrast, the NDRE map presents an even greater prevalence of green-toned zones relative to the previous stage, once more proving its enhanced performance during the latter phases of crop development.

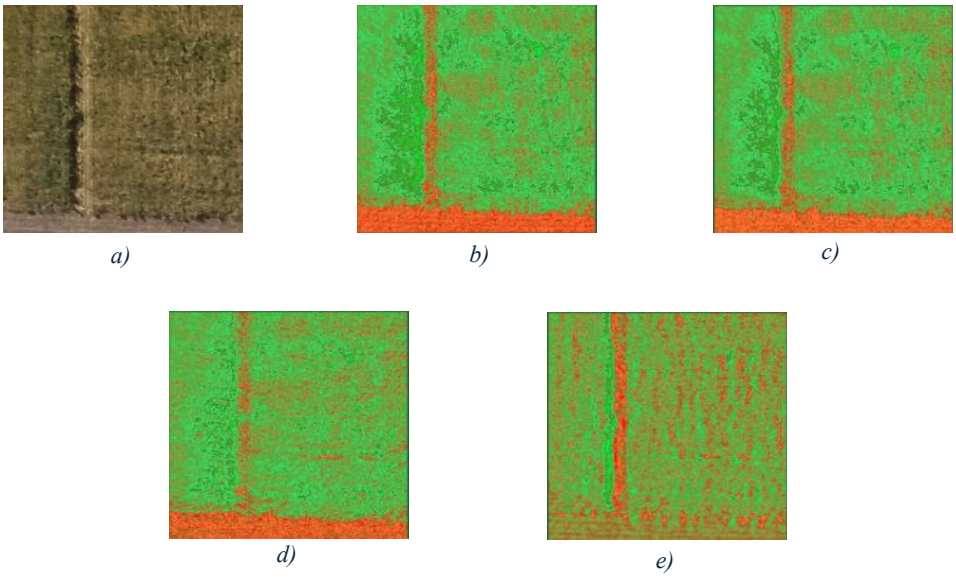

Figure 5.6 – JPEG image and index maps for 11 July from specific area analysis; a) JPEG image; b) NDVI; c) SAVI; d) GNDVI; e) NDRE

Table 5.2 presents the mean values computed by the platform for each VI for the specific region analysis, along with the qualitative assessment generated based on predefined thresholds.

Table 5.2 – Specific area analysis results

Indices		Date		
		08/06/2022	21/06/2022	11/07/2022
NDVI	Mean	0.2121	0.3574	0.1777
	Analysis	Fair	Fair	Poor
SAVI	Mean	0.0792	0.1343	0.0693
	Analysis	Very Poor	Poor	Very Poor
GNDVI	Mean	0.0487	0.1505	0.1436
	Analysis	Low	Moderate	Moderate
NDRE	Mean	-0.0280	0.0101	0.0387
	Analysis	Very Low	Very Low	Very Low

Upon analysing the results presented in the table, it is evident that the mean values increased between 8 June and 21 July across all indices, indicating an enhancement in crop vigour and chlorophyll content as the crops progress in growth. By 11 July, the mean values for NDVI, SAVI, and GNDVI either declined or remained relatively stable. This observation suggests that, as the crops reach maturity, NDVI and SAVI tend to saturate, whereas GNDVI and NDRE continue to reflect their responsiveness to chlorophyll concentration.

Similar to the whole image analysis, these results, despite having improved, are still influenced by the presence of non-crop areas, potentially affecting the crop condition assessment by the platform.

5.1.3 Masked Analysis of the Selected Area

To further mitigate the influence of non-crop areas, the previous analysis was repeated with a mask excluding zones with reflectance values of zero or below. As these correspond to non-vegetated areas, an increase in the mean values and an improved assessment are anticipated.

Figures 5.7-5.9 present the index maps generated for the three examined dates (8 June, 21 June, and 11 July 2022), corresponding to the early to late growth stages.

At this stage, after applying the mask, all the background noise caused by bare soil or non-vegetated areas was eliminated, as represented in Figure 5.7. The NDVI and SAVI maps now display no red-toned zones and close to none yellow and orange-toned zones in comparison to the unmasked analysis, indicating that the mask has effectively enhanced the visualisation of

vegetation vigour. However, the NDRE map displays several scattered regions of non-toned areas, as its sensitivity to chlorophyll remains limited during early growth stages.

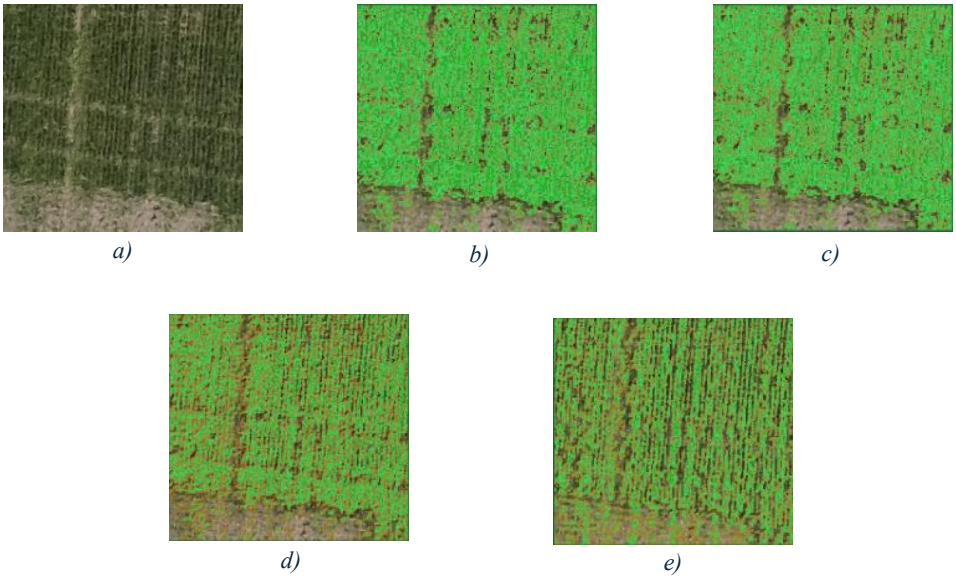

Figure 5.7 – JPEG image and index maps for 8 June from specific area with mask analysis; a) JPEG image; b) NDVI; c) SAVI; d) GNDVI; e) NDRE

During the mid-growth stage, the masking effect becomes more evident, as shown in Figure 5.8. The elimination of zero and negative pixel values emphasises the healthy crop regions, leading to predominantly green-toned areas across all indices. Compared to the unmasked analysis, the differences between indices are now more subtle, for example, NDVI and SAVI maps are nearly indistinguishable. Meanwhile, the NDRE and GNDVI maps display a stronger correlation with chlorophyll content, thereby confirming that the applied mask enhances the accuracy of vegetation assessment.

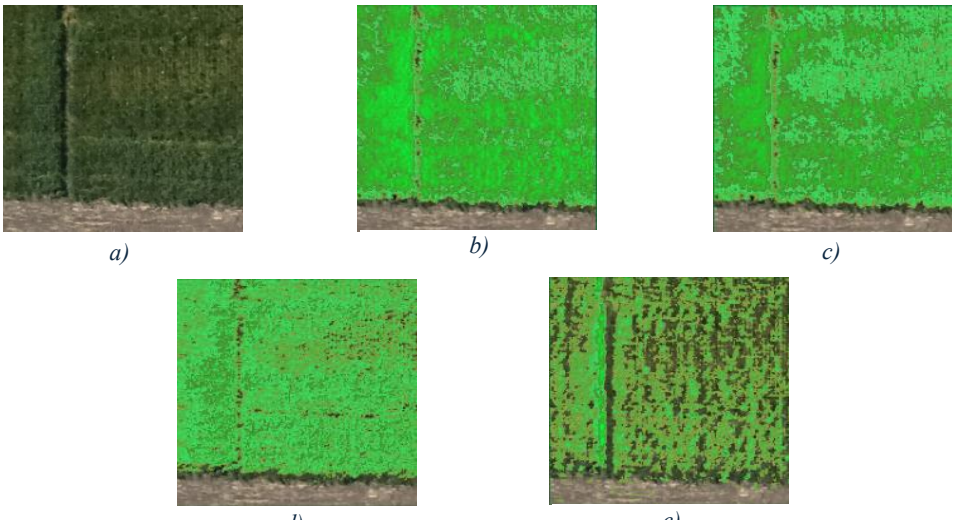

Figure 5.8 – JPEG image and index maps for 21 June from specific area with mask analysis; a) JPEG image; b) NDVI; c) SAVI; d) GNDVI; e) NDRE

In the final stage, the NDVI and SAVI maps exhibit a slight decrease in reflectance values, with the emergence of yellow to orange-toned regions, indicating a decline in vegetation vigour as the crop approaches its maturity, as displayed in Figure 5.9. At the same time, NDRE continues to demonstrate high sensitivity to chlorophyll, displaying a greater area of green zones.

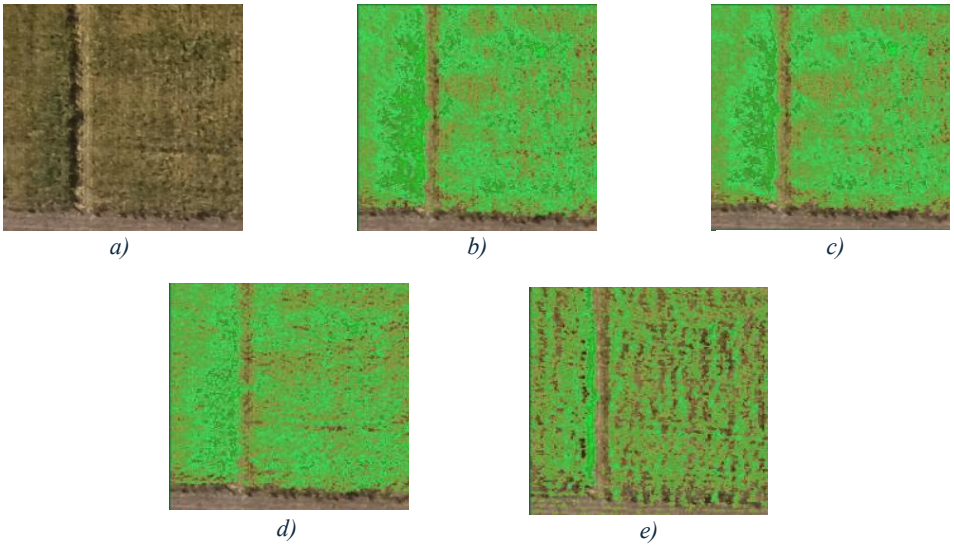

Figure 5.9 – JPEG image and index maps for 11 July from specific area with mask analysis; a) JPEG image; b) NDVI; c) SAVI; d) GNDVI; e) NDRE

Table 5.3 presents the mean values computed by the platform for each VI for the specific region with mask analysis, along with the qualitative assessment generated based on predefined thresholds.

Table 5.3 – Specific area with mask analysis results

		Date		
Indices		08/06/2022	21/06/2022	11/07/2022
NDVI	Mean	0.2956	0.4717	0.2465
	Analysis	Fair	Good	Fair
SAVI	Mean	0.1134	0.1776	0.0949
	Analysis	Poor	Poor	Very Poor
GNDVI	Mean	0.1318	0.2429	0.1994
	Analysis	Moderate	Moderate	Moderate
NDRE	Mean	0.0577	0.1040	0.1051
	Analysis	Very Low	Low	Low

Analysing the table indicates that the application of a mask to eliminate reflectance values associated with non-vegetated areas resulted in higher mean index values across all dates and

indices in comparison to previous analyses, thereby enhancing assessment outcomes. Both NDVI and SAVI exhibit increased mean values, reaching a maximum of 0.4717 and 0.1776, respectively, on 21 June, corresponding to “Good” and “Poor” classifications by the platform. By the final date, both indices demonstrate a decrease in their mean values and classifications (reverting to “Fair” and “Very Poor”), which is expected as the crops reach maturity. GNDVI and NDRE also show an increase from 8 to 21 June, reflecting an increase in chlorophyll content during the growth stages. Similar to NDVI and SAVI, GNDVI decreases by the final date. In contrast, NDRE exhibits a slight increase, maintaining its “Low” classification, thereby evidencing its sensitivity and reliability in monitoring crop health during later growth phases.

5.2 Comparative Discussion

Figures 5.4–5.7 present a comparative visualisation of the mean vegetation index values obtained from the three analysis approaches (whole image, specific area, and specific area with masking) across all acquisition dates. These figures highlight the temporal evolution of each index and enable a direct comparison of the impact of spatial filtering on vegetation assessment results.

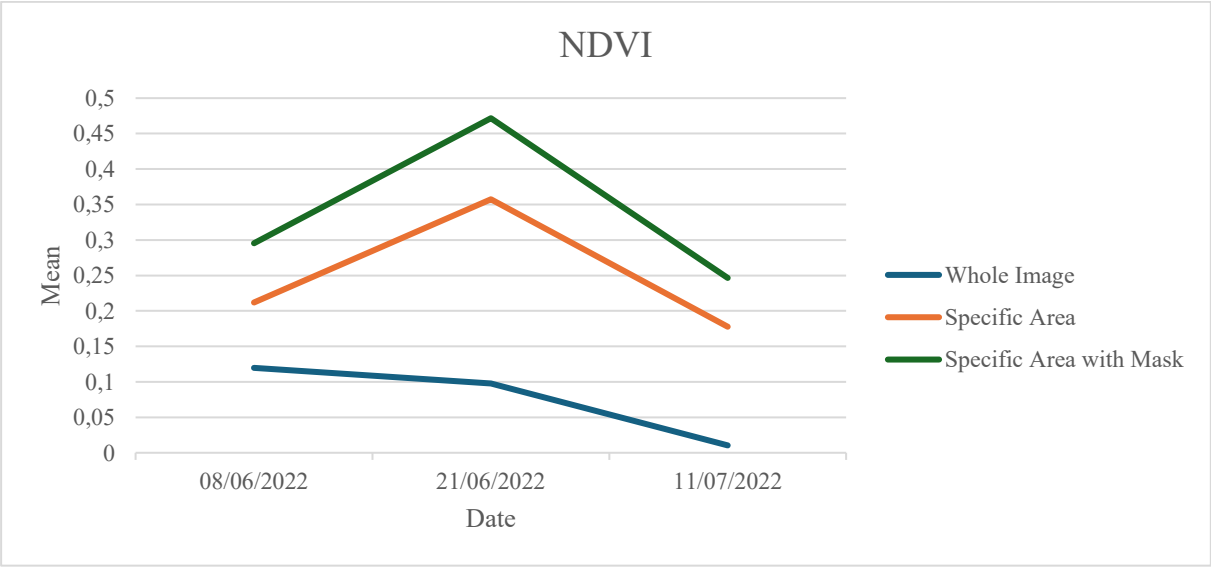

Figure 5.10 – Temporal evolution of mean NDVI values for the whole image, specific area, and specific area with masking across the three acquisition dates

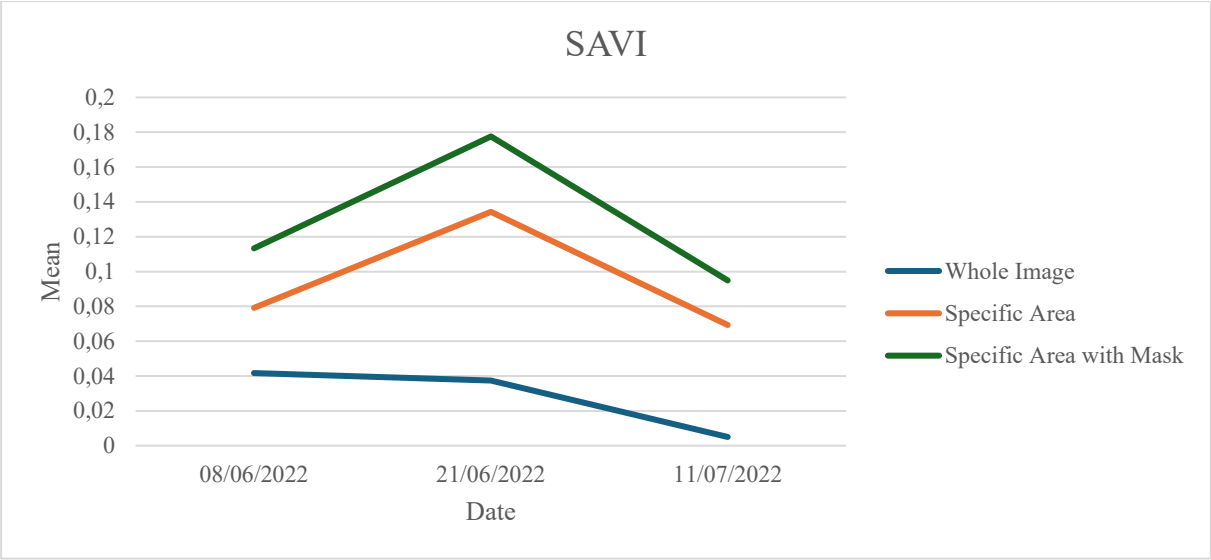

Figure 5.11 – Temporal evolution of mean SAVI values for the whole image, specific area, and specific area with masking across the three acquisition dates

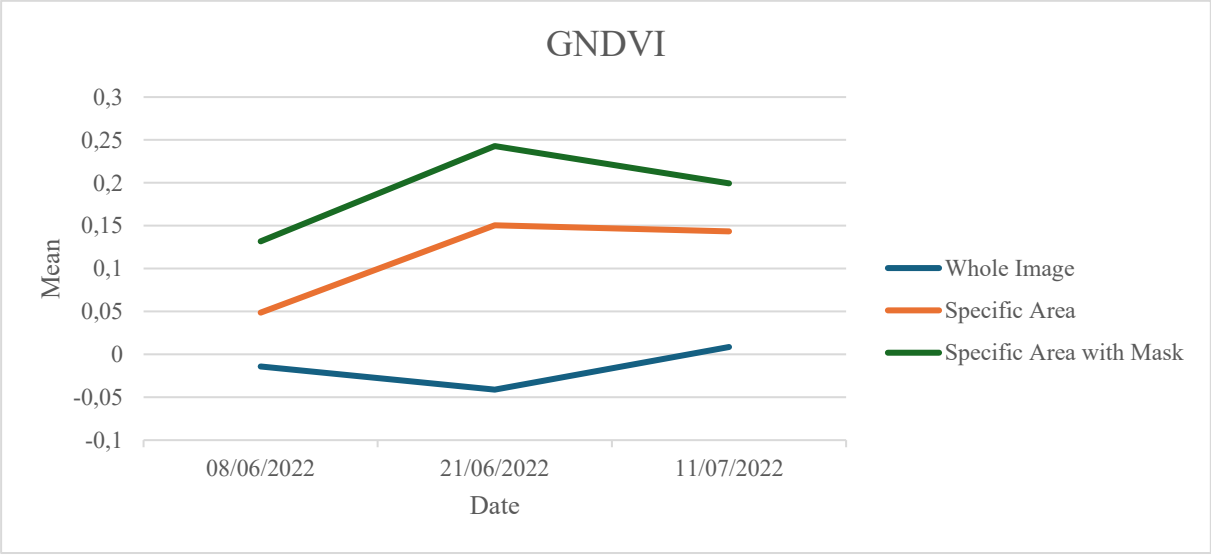

Figure 5.12 – Temporal evolution of mean GNDVI values for the whole image, specific area, and specific area with masking across the three acquisition dates

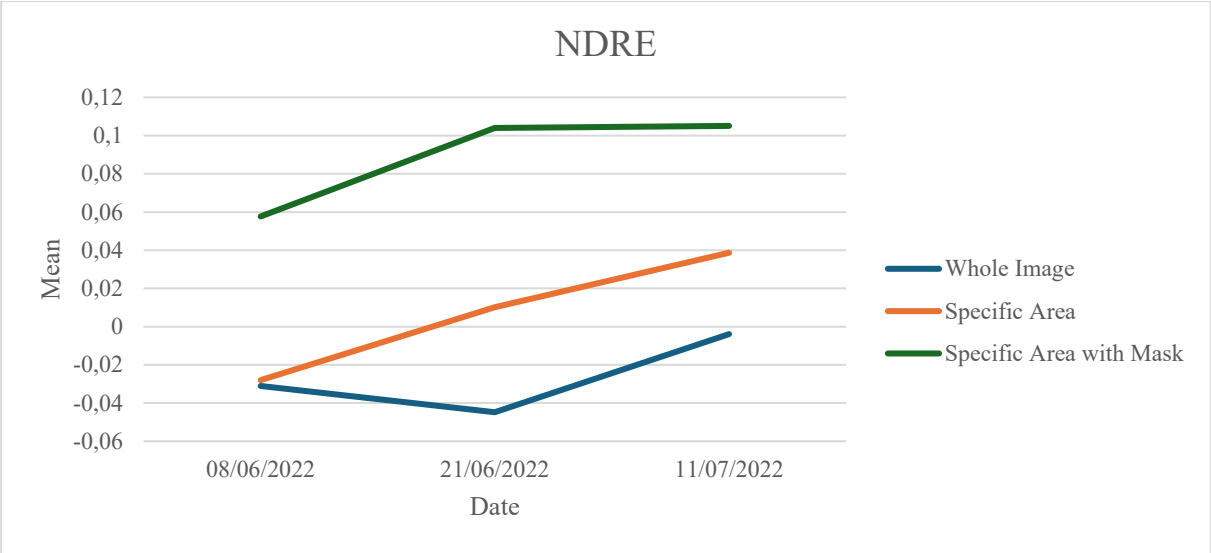

Figure 5.13 – Temporal evolution of mean NDRE values for the whole image, specific area, and specific area with masking across the three acquisition dates

Comparing the results obtained from the three analyses, it is possible to observe a clear improvement in the mean index values and their associated classifications. Going from the whole image to the masked analysis demonstrates how excluding non-vegetated zones significantly influences the overall outcomes. In the initial analysis, the mean index values consistently remained low, resulting in classifications such as "Very Poor" or "Non-Vegetated." When the analysis was confined to a specific area, a notable increase in the mean index values was already noticed. Still, it was when the mask was applied that these values reached their peak. This once again demonstrates the impact of background elements on the results, thereby contributing to a reduction in assessment accuracy.

Although the values show an improvement over time, they remain within the lower qualitative classes defined by the adopted classification thresholds across all vegetation indices. This difference may be attributed to external factors such as image resolution, sensor calibration, or atmospheric conditions during image acquisition, which can result in decreased spectral reflectance consistency. Future analyses may be improved by capturing imagery at lower UAV flight altitudes to enhance image resolution and by implementing additional atmospheric correction procedures to mitigate these influences even further.

As for the performance of the used indices, NDVI and SAVI displayed similar behaviour, effectively capturing the overall vigour of the vegetation. Both indices reached their peak during the mid-growth stage, indicating optimal canopy development. However, SAVI, despite exhibiting lower values due to soil adjustment, continued to reflect NDVI's temporal pattern, thereby enhancing its reliability under conditions of partial vegetation cover. GNDVI, although

expected to respond more strongly only during the later stages of growth, maintained consistent performance throughout all stages. On the other hand, NDRE confirmed its superior sensitivity during the later growth stages, as evidenced by increased mean values when other indices declined, thanks to its capacity to penetrate more deeply into the vegetation and detect subtle variations in chlorophyll concentration.

In conclusion, the utilisation of spatial filtering techniques, such as masking, enhances the precision of vegetation assessments. By excluding the influence of non-vegetated areas, the analysis more accurately represents actual crop conditions, thereby reducing errors across the different growth stages.

CHAPTER 6

Conclusion and Future Work

Agriculture remains one of the most essential sectors for global food production; however, it faces numerous challenges, including population growth, climate change, and resource scarcity. These issues have increased environmental variability, reduced water resources, and limited arable land, thereby affecting agricultural productivity and sustainability.

The emergence of PA provides a practical solution to these challenges by facilitating data-driven management of crops and resources. In this context, multispectral imaging has demonstrated considerable viability, supplying both spatial and spectral data that improve the oversight of crop development and vegetation health.

The main objective of this dissertation was to develop a platform capable of processing and analysing multispectral imagery, enabling the generation of quantitative assessments of crop growth and vigour through VIs.

The following sections summarise the main conclusions obtained throughout the study, its limitations and potential future work.

6.1 Conclusions

The following conclusions summarise the primary outcomes gained from the implementation and validation of the developed platform for multispectral image analysis. Additionally, they seek to address the research questions delineated in Chapter 1, which directed the progression of this dissertation.

Firstly, the developed research demonstrated that the use of multispectral imaging in agricultural monitoring enhances accuracy when compared to the traditional, manual methods. By making use of the spectral bands, it becomes possible to obtain a more detailed assessment of the crop's physiological conditions, such as vegetation density and chlorophyll content. These data allow farmers not only to monitor crop health but also to gain new insights regarding vegetation development and stress levels, which would be difficult to determine through visual inspection alone.

Furthermore, the use of VIs, such as NDVI, SAVI, GNDVI, and NDRE, was determined to be crucial for assessing crop conditions throughout various growth stages. Each index demonstrated specific strengths, for instance, NDVI and SAVI exhibited greater consistency during the early to mid-growth stages. In contrast, GNDVI and NDRE, due to their higher sensitivity to chlorophyll and canopy structure, were more effective during the later stages.

Continuing, by using spatial filtering and masking techniques, it was possible to significantly reduce the influence of non-crop elements, thereby producing more precise and stable vegetation assessments. Consequently, it can be concluded that mean index values derived from unfiltered imagery may result in misleading evaluations of crop vigour due to the influence of irrelevant pixels. Additionally, it emphasised the importance of data preprocessing in order to improve the precision of the results.

Regarding the environmental and economic implications, the platform facilitates a more efficient and sustainable approach to crop monitoring, being capable of early detection of stress conditions, nutrient deficiencies, or irregular growth patterns. This results in a reduction of field interventions, thereby diminishing resource waste and operational costs.

From an operational perspective, the process of importing, organising, and analysing multispectral images was greatly simplified with the developed platform. By offering a user-friendly interface and an intuitive workflow, a once complex process has become straightforward and accessible even to non-expert users. The integration of local storage via an SQLite database further enhances its usability in agricultural regions with limited internet access.

In conclusion, this study verified the effectiveness of a multispectral image analysis platform designed for precision agriculture and demonstrated how integrating VIs can help farmers monitor crops more efficiently. This result highlights the potential of multispectral imaging as a basis for future developments in automated image analysis, real-time field monitoring, and decision support systems in modern agriculture.

6.2 Limitations

Throughout the development of this dissertation, some limitations were encountered. These will be addressed in the current section.

One of the primary issues faced was the lack of available multispectral datasets that conformed to the platform's intended applications and technical specifications. Consequently, it was imperative to utilise a dataset that, while suitable for testing the platform's functionalities, offered a lower spatial resolution than optimal for comprehensive vegetation analysis. This limitation may have impacted the precision of the computed VIs.

Another possible limitation could be the influence of atmospheric conditions during image acquisition. Although the image acquisition of the chosen dataset was performed under similar atmospheric conditions across all flight sessions, the images did not undergo previous atmospheric correction procedures; variations in humidity, illumination, and haze may have caused spectral distortions, which could have affected the consistency of reflectance between dates, thereby contributing to the relatively low VI values observed in Chapter 5.

6.3 Future Work

To enhance the platform's functionalities, usability, and analytical capabilities, several potential future developments and improvements have been identified.

One of these enhancements involves the integration of cloud connectivity into the platform. By establishing a connection to an online database, the platform would enable users to upload their multispectral imagery, thereby facilitating access from multiple devices. Furthermore, user authentication and registration functionalities could also be implemented to ensure secure data management and personal data access control.

Currently, the platform requires users to download the acquired images from the UAV onto a computer and subsequently upload them for analysis. By integrating the platform directly into the UAV, this intermediate step could be eliminated, enabling real-time vegetation assessment during flight. Such integration would not only improve operational efficiency but also allow for iterative analysis and on-the-fly adjustment of data acquisition when preliminary results are deemed insufficient, thereby increasing system autonomy and suitability for large-scale agricultural operations.

Another interesting improvement would involve the integration of machine learning algorithms to refine image pre-processing and analysis processes. These algorithms could be employed to automatically detect and eliminate non-crop regions, thereby further minimising their influence on VI outcomes. Furthermore, beyond filtering capabilities, machine learning

algorithms could provide more refined and data-driven evaluations, replacing the platform's current mean-value methodology.

Lastly, the platform's capabilities could be expanded by broadening its support to include additional image types, such as hyperspectral, thermal, or RGB images. Incorporating these types would enable the platform to analyse a wider range of agricultural metrics, including disease detection, thermal stress assessment, and water content analysis. This enhancement would deepen the system's analytical capabilities and extend its applicability to various crops and agricultural environments.

References

[1] K. Rose, S. Eldridge, and L. Chapin, “The Internet of Things: An Overview Understanding the Issues and Challenges of a More Connected World,” 2015.

[2] A. Bassi *et al.*, “Enabling Things to Talk Designing IoT solutions with the IoT Architectural Reference Model,” 2013. doi: 10.1007/978-3-642-40403-0.

[3] R. Sadigov, “Rapid Growth of the World Population and Its Socioeconomic Results,” *Scientific World Journal*, vol. 2022, 2022, doi: 10.1155/2022/8110229.

[4] K. Abbass, M. Z. Qasim, H. Song, M. Murshed, H. Mahmood, and I. Younis, “A review of the global climate change impacts, adaptation, and sustainable mitigation measures,” *Environmental Science and Pollution Research*, vol. 29, no. 28. Springer Science and Business Media Deutschland GmbH, Jun. 01, 2022. doi: 10.1007/s11356-022-19718-6.

[5] X. Liu, W. Liu, Q. Tang, B. Liu, Y. Wada, and H. Yang, “Global Agricultural Water Scarcity Assessment Incorporating Blue and Green Water Availability Under Future Climate Change,” *Earth’s Future*, vol. 10, no. 4, Apr. 2022, doi: 10.1029/2021EF002567.

[6] S. Zhao and M. Yin, “Change of urban and rural construction land and driving factors of arable land occupation,” *PLoS ONE*, vol. 18, no. 5, May 2023, doi: 10.1371/journal.pone.0286248.

[7] S. Tan *et al.*, “Characteristics and influencing factors of chemical fertilizer and pesticide applications by farmers in hilly and mountainous areas of Southwest, China,” *Ecological Indicators*, vol. 143, Oct. 2022, doi: 10.1016/j.ecolind.2022.109346.

[8] U. Shafi, R. Mumtaz, J. García-Nieto, S. A. Hassan, S. A. R. Zaidi, and N. Iqbal, “Precision agriculture techniques and practices: From considerations to applications,” *Sensors (Switzerland)*, vol. 19, no. 17. MDPI AG, Sep. 01, 2019. doi: 10.3390/s19173796.

[9] R. G. Guntara, M. R. Nugraha, and M. D. A. Ridlo, “Web-Based Counseling Skills Evaluation Information System Using Design Science Research Methodology (DSRM) Approach,” *International Journal of Advances in Data and Information Systems*, vol. 4, no. 2, Sep. 2023, doi: 10.25008/ijadis.v4i2.1288.

[10] M. Mondal and Z. Rehena, “IoT Based Intelligent Agriculture Field Monitoring System,” 2018, doi: 10.1109/CONFLUENCE.2018.8442535.

[11] S. Tenzin, S. Siyang, T. Pobkrut, and T. Kerdcharoen, “Low Cost Weather Station for Climate-Smart Agriculture,” 2017, doi: 10.1109/KST.2017.7886085.

[12] A. Triantafyllou, D. C. Tsouros, P. Sarigiannidis, and S. Bibi, “An Architecture model for Smart Farming,” 2019, doi: 10.1109/DCOSS.2019.00081.

[13] A. D. Boursianis *et al.*, “Smart Irrigation System for Precision Agriculture - The ARETHOU5A IoT Platform,” *IEEE Sensors Journal*, vol. 21, no. 16, Aug. 2021, doi: 10.1109/JSEN.2020.3033526.

[14] S. Roy, S. Member, S. Misra, S. Member, N. Singh Raghuwanshi, and S. K. Das, “AgriSens: IoT-Based Dynamic Irrigation Scheduling System for Water Management of Irrigated Crops,” *IEEE INTERNET OF THINGS JOURNAL*, vol. 8, no. 6, 2021, doi: 10.1109/JIOT.2020.3036126.

[15] A. Al-Naji, A. B. Fakhri, S. K. Gharghan, and J. Chahl, “Soil color analysis based on a RGB camera and an artificial neural network towards smart irrigation: A pilot study,” *Heliyon*, vol. 7, no. 1, Jan. 2021, doi: 10.1016/j.heliyon.2021.e06078.

[16] M. Badreldeen, M. A. Ragab, A. Sedhom, W. M. Mamdouh, and M. Ali Ragab, “IoT based Smart Irrigation System,” *International Journal of Industry and Sustainable Development (IJISD)*, vol. 3, no. 1, 2022, doi: 10.21608/ijisd.2022.148007.1021.

[17] J. Sun, A. M. Abdulghani, M. A. Imran, and Q. H. Abbasi, “IoT Enabled Smart Fertilization and Irrigation Aid for Agricultural Purposes,” in *ACM International Conference Proceeding Series*, Association for Computing Machinery, Apr. 2020. doi: 10.1145/3398329.3398339.

[18] J. B. Ristaino *et al.*, “The persistent threat of emerging plant disease pandemics to global food security,” May 2021, doi: 10.1073/pnas.2022239118.

[19] S. Ghosal, D. Blystone, A. K. Singh, B. Ganapathysubramanian, A. Singh, and S. Sarkar, “An explainable deep machine vision framework for plant stress phenotyping,” *Proceedings of the National Academy of Sciences of the United States of America*, vol. 115, no. 18, May 2018, doi: 10.1073/pnas.1716999115.

[20] L. C. Ngugi, M. Abelwahab, and M. Abo-Zahhad, “Recent advances in image processing techniques for automated leaf pest and disease recognition – A review,” *Information Processing in Agriculture*, vol. 8, no. 1. China Agricultural University, Mar. 01, 2021. doi: 10.1016/j.inpa.2020.04.004.

[21] J. Su *et al.*, “Wheat yellow rust monitoring by learning from multispectral UAV aerial imagery,” *Computers and Electronics in Agriculture*, vol. 155, Dec. 2018, doi: 10.1016/j.compag.2018.10.017.

[22] A. di Nisio, F. Adamo, G. Acciani, and F. Attivissimo, “Fast detection of olive trees affected by xylella fastidiosa from uavs using multispectral imaging,” *Sensors (Switzerland)*, vol. 20, no. 17, Sep. 2020, doi: 10.3390/s20174915.

[23] M. Kerkech, A. Hafiane, and R. Canals, “VddNet: Vine disease detection network based on multispectral images and depth map,” *Remote Sensing*, vol. 12, no. 20, Oct. 2020, doi: 10.3390/rs12203305.

[24] S. Cubero, E. Marco-noales, N. Aleixos, S. Barbé, and J. Blasco, “Robhortic: A field robot to detect pests and diseases in horticultural crops by proximal sensing,” *Agriculture (Switzerland)*, vol. 10, no. 7, Jul. 2020, doi: 10.3390/agriculture10070276.

[25] J. S. Duhan, R. Kumar, N. Kumar, P. Kaur, K. Nehra, and S. Duhan, “Nanotechnology: The new perspective in precision agriculture,” *Biotechnology Reports*, vol. 15. Elsevier B.V., Sep. 01, 2017. doi: 10.1016/j.btre.2017.03.002.

[26] X. Pei, K. A. Sudduth, K. S. Veum, and M. Li, “Improving in-situ estimation of soil profile properties using a multi-sensor probe,” *Sensors (Switzerland)*, vol. 19, no. 5, Mar. 2019, doi: 10.3390/s19051011.

[27] N. Nair, A. A. V. Akshaya, and J. Joseph, “An In-Situ Soil pH Sensor With Solid Electrodes,” *IEEE Sensors Letters*, vol. 6, no. 8, Aug. 2022, doi: 10.1109/LSENS.2022.3194200.

[28] A. Matese *et al.*, “Intercomparison of UAV, aircraft and satellite remote sensing platforms for precision viticulture,” *Remote Sensing*, vol. 7, no. 3, 2015, doi: 10.3390/rs70302971.

[29] D. D. Sweet, S. B. Tirado, N. M. Springer, C. N. Hirsch, and C. D. Hirsch, "Opportunities and challenges in phenotyping row crops using drone-based RGB imaging," *Plant Phenome Journal*, vol. 5, no. 1, 2022, doi: 10.1002/ppj2.20044.

[30] J. Giménez-Gallego, J. D. González-Teruel, F. Soto-Valles, M. Jiménez-Buendía, H. Navarro-Hellín, and R. Torres-Sánchez, "Intelligent thermal image-based sensor for affordable measurement of crop canopy temperature," *Computers and Electronics in Agriculture*, vol. 188, Sep. 2021, doi: 10.1016/j.compag.2021.106319.

[31] V. Swaminathan, J. A. Thomasson, R. G. Hardin, N. Rajan, and R. Raman, "Selection of appropriate multispectral camera exposure settings and radiometric calibration methods for applications in phenotyping and precision agriculture," *Plant Phenome Journal*, vol. 7, no. 1, Dec. 2024, doi: 10.1002/ppj2.70000.

[32] T. B. Shahi, C. Y. Xu, A. Neupane, and W. Guo, "Machine learning methods for precision agriculture with UAV imagery: a review," *Electronic Research Archive*, vol. 30, no. 12, 2022, doi: 10.3934/era.2022218.

[33] R. Guebsi, S. Mami, and K. Chokmani, "Drones in Precision Agriculture: A Comprehensive Review of Applications, Technologies, and Challenges," *Drones*, vol. 8, no. 11. Multidisciplinary Digital Publishing Institute (MDPI), Nov. 01, 2024. doi: 10.3390/drones8110686.

[34] N. Delavarpour, C. Koparan, J. Nowatzki, S. Bajwa, and X. Sun, "A technical study on UAV characteristics for precision agriculture applications and associated practical challenges," *Remote Sensing*, vol. 13, no. 6. MDPI AG, Mar. 02, 2021. doi: 10.3390/rs13061204.

[35] Candiago, S., Remondino, F., De Giglio, M., Dubbini, M., & Gattelli, M. (2015). Evaluating Multispectral Images and Vegetation Indices for Precision Farming Applications from UAV Images. *Remote Sensing*, *7*(4), 4026-4047. https://doi.org/10.3390/rs70404026

[36] DJI. (n.d.). *P4 Multispectral*. Retrieved September 28, 2025, from https://ag.dji.com/p4-multispectral

[37] Radočaj, D., Šiljeg, A., Marinović, R., & Jurišić, M. (2023). State of Major Vegetation Indices in Precision Agriculture Studies Indexed in Web of Science: A Review. Agriculture, 13(3), 707. https://doi.org/10.3390/agriculture13030707

[38] Vidican, R., Mălinaș, A., Ranta, O., Moldovan, C., Marian, O., Ghețe, A., Ghișe, C. R., Popovici, F., & Cătunescu, G. M. (2023). Using Remote Sensing Vegetation Indices for the Discrimination and Monitoring of Agricultural Crops: A Critical Review. *Agronomy*, *13*(12), 3040. https://doi.org/10.3390/agronomy13123040

[39] Huang, S., Tang, L., Hupy, J.P. *et al.* A commentary review on the use of normalized difference vegetation index (NDVI) in the era of popular remote sensing. *J. For. Res.* **32**, 1–6 (2021). https://doi.org/10.1007/s11676-020-01155-1

[40] Plant optics: Underlying mechanisms in remotely sensed signals for phenotyping applications. (2023). *Aob Plants*. https://doi.org/10.1093/aobpla/plad039

[41] Pettorelli N, Ryan S, Mueller T, Bunnefeld N, Jedrzejewska B, Lima M, Kausrud K (2011) The Normalized Difference Vegetation Index (NDVI): unforeseen successes in animal ecology. Clim Res 46:15-27 https://doi.org/10.3354/cr00936

[42] Ding, Y., Zheng, X., Zhao, K., Xin, X., & Liu, H. (2016). Quantifying the Impact of $NDVI_{soil}$ Determination Methods and $NDVI_{soil}$ Variability on the Estimation of Fractional Vegetation Cover in Northeast China. *Remote Sensing*, *8*(1), 29. https://doi.org/10.3390/rs8010029

[43] Huete, A. R. (1988). A soil-adjusted vegetation index (SAVI). *Remote Sensing of Environment*, *25*(3), 295–309. https://doi.org/10.1016/0034-4257(88)90106-x

[44] Tucker, C. J. (1979). Red and photographic infrared linear combinations for monitoring vegetation. *Remote Sensing of Environment*, *8*(2), 127–150. https://doi.org/10.1016/0034-4257(79)90013-0

[45] Kumar, B. P., Babu, K. R., M. Rajasekhar, & Ramachandra, M. (2022). Assessment of the Visual Disaster of Land Degradation and Desertification Using TGSI, SAVI, and NDVI Techniques. *CRC Press EBooks*, 261–279. https://doi.org/10.1201/9781003147107-18

[46] Rondeaux, G., Steven, M., & Baret, F. (1996). Optimization of soil-adjusted vegetation indices. *Remote Sensing of Environment*, *55*(2), 95–107. https://doi.org/10.1016/0034-4257(95)00186-7

[47] Qi, J., Chehbouni, A., Huete, A. R., Kerr, Y. H., & Sorooshian, S. (1994). A modified soil adjusted vegetation index. *Remote Sensing of Environment*, *48*(2), 119–126. https://doi.org/10.1016/0034-4257(94)90134-1

[48] Auravant. (n.d.). *Vegetation indices and their interpretation: NDVI, GNDVI, MSAVI2, NDRE, and NDWI*. Auravant. https://www.auravant.com/en/articles/precision-agriculture/vegetation-indices-and-their-interpretation-ndvi-gndvi-msavi2-ndre-and-ndwi/

[49] Nițu, A., Florea, C., Ivanovici, M., & Racoviteanu, A. (2025). NDVI and Beyond: Vegetation Indices as Features for Crop Recognition and Segmentation in Hyperspectral Data. *Sensors*, *25*(12), 3817. https://doi.org/10.3390/s25123817

[50] Mangewa, L. J., Ndakidemi, P. A., Alward, R. D., Kija, H. K., Bukombe, J. K., Nasolwa, E. R., & Munishi, L. K. (2022). Comparative Assessment of UAV and Sentinel-2 NDVI and GNDVI for Preliminary Diagnosis of Habitat Conditions in Burunge Wildlife Management Area, Tanzania. *Earth*, *3*(3), 769-787. https://doi.org/10.3390/earth3030044

[51] Boiarskii, B. (2019). Comparison of NDVI and NDRE Indices to Detect Differences in Vegetation and Chlorophyll Content. *JOURNAL of MECHANICS of CONTINUA and MATHEMATICAL SCIENCES*, *spl1*(4). https://doi.org/10.26782/jmcms.spl.4/2019.11.00003

[52] Voitik, A., Kravchenko, V., Olexandr Pushka, Tetyana Kutkovetska, Taras Shchur, & Sławomir Kocira. (2023). Comparison of NDVI, NDRE, MSAVI and NDSI Indices for Early Diagnosis of Crop Problems. *Agricultural Engineering/Inżynieria Rolnicza*, *27*(1), 47–57. https://doi.org/10.2478/agriceng-2023-0004

[53] Kurbanov, R. K., & Zakharova, N. I. (2020). Application of Vegetation Indexes to Assess the Condition of Crops. *Agricultural Machinery and Technologies*, *14*(4), 4–11. https://doi.org/10.22314/2073-7599-2020-14-4-4-11

[54] Magney, T. S., Jan, & Vierling, L. A. (2016). Mapping wheat nitrogen uptake from RapidEye vegetation indices. *Precision Agriculture*, *18*(4), 429–451. https://doi.org/10.1007/s11119-016-9463-8

[55] Maulit, A., Nugumanova, A., Apayev, K., Baiburin, Y., & Sutula, M. (2023). A multispectral UAV imagery dataset of wheat, soybean and barley crops in East Kazakhstan. *Data*, *8*(5), 88. https://doi.org/10.3390/data8050088